Hong Kong

MEDICAL
JOURNAL

香港醫學雜誌

The official publication of the
Hong Kong Academy of Medicine
and the Hong Kong Medical Association

Research Fund for the Control of Infectious Diseases

Research Dissemination Reports

控制傳染病研究基金

研究成果報告

Respiratory Infectious Diseases
呼吸道感染疾病

Vector-Borne Diseases
病媒傳播疾病

HONG KONG MEDICAL JOURNAL
香 港 醫 學 雜 誌

Vol 18 No 1 February 2012
Supplement 2

Research Fund for the Control of Infectious Diseases

Research Dissemination Reports

VECTOR-BORNE DISEASES

EDITORIAL

Dissemination reports are concise informative reports of health-related research supported by funds administered by the Food and Health Bureau, namely the *Research Fund for the Control of Infectious Diseases* (RFCID), the *Health and Health Services Research Fund* (HHSRF), and the *Health Services Research Fund* (HSRF). In this edition, 12 dissemination reports of RFCID-funded projects related to respiratory infectious diseases and vector-borne diseases are presented. In particular, three projects are highlighted due to their potentially significant findings, impact on health care delivery and practice, and/or contribution to health policy formulation in Hong Kong.

Influenza vaccination for older people (age ≥65 years) in the community may reduce hospitalisation by 25 to 39% and overall mortality by 39 to 75% during influenza seasons. Most of these data are derived from studies in temperate regions with well-defined influenza seasons. The effectiveness of influenza vaccination in tropical and sub-tropical regions, where influenza may circulate at lower levels throughout the year, is less known. To determine whether influenza vaccination decreased hospitalisation and mortality, Schooling et al[1] examined a cohort of Elderly Health Centres in Hong Kong. In the influenza season, influenza vaccination reduced all-cause mortality by half and cardiorespiratory hospitalisation by a quarter. However, the authors caution that the extent to which influenza vaccination actually protects older people from serious morbidity and mortality needs to be confirmed in appropriately designed studies.

In 2005, investigators in Hong Kong discovered a novel human coronavirus (HCoV) named HKU1. In an attempt to discover an animal reservoir for it, Yuen et al[2] discovered a novel bat coronavirus closely related to the coronavirus causing severe acute respiratory syndrome (SARS). Complete genome sequencing and phylogenetic analysis showed that this bat-SARS-CoV formed a distinct cluster with SARS-CoV as a group distantly related to other known coronaviruses. This suggests that HCoV-HKU1 is closely related to SARS-CoV from humans and civets and that bats are the likely animal reservoir of SARS-CoV-like viruses. The authors suggest that continuous surveillance for coronaviruses in these flying mammals is necessary to assess their potential threat to human health.

Acute respiratory tract infections account for considerable morbidity and mortality in humans. Human coronavirus (HCoV) NL63 was discovered in 2004. Leung et al[3] investigated the seasonality and epidemiology of HCoV-NL63 in local children and characterised the genetic diversity of local HCoV-NL63 isolates. The four major human coronaviruses were detected in 2.5% of 2982 local children hospitalised for acute respiratory infections from 2005 to 2007, of which 0.6% were attributable to HCoV-NL63. The peak season for HCoV-NL63 infection was autumn (September to October). HCoV-NL63 infection was associated with younger age, croup, febrile convulsion, and acute gastroenteritis. Such disease associations were not found with the other three HCoVs. With a few exceptions, most local isolates of HCoV-NL63 were closely related to the prototype strain from the Netherlands.

We hope you will enjoy this selection of research dissemination reports. Electronic copies can be downloaded from the Research Fund Secretariat website (**http://www.fhb.gov.hk/grants**). Researchers interested in the funds administered by the Food and Health Bureau may also visit the website for detailed information about application procedures.

Supplement co-editors

Dr Jenny Lam
Associate Consultant
(Research Office)
Food and Health Bureau

Dr Richard A Collins
Scientific Review Director
(Research Office)
Food and Health Bureau

References

1. Schooling CM, McGhee SM, Cowling BJ, et al. Influenza vaccination and hospitalisation in Elderly Health Centres. Hong Kong Med J 2012;18(Suppl 2):4-7.
2. Yuen KY, Lau KP, Woo CY. Wild animal surveillance for coronavirus HKU1 and potential variants of other coronaviruses. Hong Kong Med J 2012;18(Suppl 2):25-6.
3. Leung TF, Chan KS, Wong WK, Ip M, Cheng WT, Ng PC. Human coronavirus NL63 in children: epidemiology, disease spectrum, and genetic diversity. Hong Kong Med J 2012;18(Suppl 2):27-30.

CM Schooling 舒菱
SM McGhee 麥潔儀
BJ Cowling 高本恩
GN Thomas
WM Chan 陳慧敏
KS Ho 何建生
VCW Wong 黃譚智媛
GM Leung 梁卓偉

Key Messages

1. A cohort of Elderly Health Centres was examined to determine whether influenza vaccination decreased hospitalisation and mortality.
2. In the influenza season, influenza vaccination reduced all-cause mortality by half and cardiorespiratory hospitalisation by a quarter. The extent to which influenza vaccination protects older people from serious morbidity and mortality needs to be confirmed in appropriately designed studies, so that scarce health care resources can be used effectively.

Department of Community Medicine and School of Public Health, The University of Hong Kong
CM Schooling, SM McGhee, BJ Cowling, GN Thomas, GM Leung
Department of Health, Hong Kong
WM Chan, KS Ho
Hospital Authority, Hong Kong
VCW Wong

RFCID project number: 04050182

Principal applicant and corresponding author:
Dr C Mary Schooling
Department of Community Medicine and School of Public Health, Li Ka Shing Faculty of Medicine, 21 Sassoon Road, Pokfulam, Hong Kong SAR, China
Tel: (852) 3906 2032
Fax: (852) 3520 1945
Email: cms1@hkucc.hku.hk

Influenza vaccination and hospitalisation in Elderly Health Centresz

Introduction

In Hong Kong, influenza-associated morbidity and mortality are similar to those in temperate climates.[1] The World Health Organization (WHO) reports that influenza vaccination for older people (age ≥65 years) in the community may reduce hospitalisation by 25 to 39% and overall mortality by 39 to 75% during influenza seasons. These estimates are substantiated by reviews and meta-analyses,[2] but are increasingly controversial. First, it is difficult to reconcile them with seasonal influenza-related mortality,[3] because such a reduction in mortality in older people during the main influenza season could prevent more deaths than are caused by influenza. Second, the plausibility of influenza vaccination being most effective at preventing non-specific outcomes (such as all-cause mortality) and least effective at preventing influenza has been questioned.[2] Third, concerns have been raised as to whether the people most liable to die from influenza, ie the very old, are capable of mounting an effective immunological response to the vaccine.

Effectiveness of influenza vaccine against influenza or influenza-like illness has been assessed in older people in five randomised control trials,[2] whereas such effectiveness against hospitalisation and mortality has been obtained from observational studies comparing older people who volunteered for influenza vaccination with those who did not. This may create biases if those vaccinated and unvaccinated are systemically different. Observational evidence can be soundly based, but is not always confirmed in trials. Effectiveness of influenza vaccination in tropical and sub-tropical regions is less known, because most such research comes from temperate climates with a well-defined influenza season, whereas in tropical and sub-tropical regions, influenza may circulate at lower levels throughout the year.[4] Subsequent to the severe acute respiratory syndrome (SARS) outbreak in Hong Kong in 2003, influenza vaccination has become more common among community-dwelling older people. Previously, influenza vaccination was only provided to older people living in institutions. This change enables examination of influenza vaccination in reducing morbidity and mortality of older people living in the community.

Methods

This study was conducted from 15 June 2006 to 15 September 2007. Since July 1998, 18 Elderly Health Centres have been established to deliver health examinations and primary care services for older adults by the Department of Health of Hong Kong. All elderly residents in Hong Kong aged ≥65 years were encouraged to enrol. This study covered all community-dwelling enrolees from July 1998 to December 2001. More women enrolled than men; otherwise the enrolees were similar to the general elderly population in terms of age, socio-economic status, current smoking status, and hospital use. Record linkage by unique Hong Kong identity card numbers was used to obtain all deaths and admissions to public hospitals, which accounts for almost 95% of hospital use by older people.

Multivariable negative binomial and Poisson regression was used to compare the risk of hospital admission or death in this cohort in the 2 years prior to SARS

(2001/2) and the 2 years after SARS (2004/5). Relative risks (incident rate ratios) with 95% confidence intervals were reported. The exposure was the length of time the Elderly Health Centre client was potentially exposed to influenza infection in 2001-2 and/or 2004-5, ie the duration of survival in each period. Exposure time started at the beginning of the relevant period, but at least one year after enrolment, because an older person capable of attending the Elderly Health Centre is unlikely to die immediately from a complication of influenza. As the same person may have exposure in both periods, which artefactually reduces the variance, we used the average estimates and standard errors from 100 different random splits of the cohort into two equally sized halves. Patient age, sex, education levels, and smoking status were adjusted for.

Different associations in potentially more vulnerable groups, such as older people, from the heterogeneity of effect across strata and the significance of interaction terms were examined, as were different associations in people receiving financial assistance (CSSA) or in poor health, because these people might be more likely to have been vaccinated. Admission and mortality in the high and low influenza seasons were compared. Based on surveillance data,[4] the influenza high season was defined as 3 months from 1 February in 2001, 2004, and 2005 and from 1 January in 2002. The influenza low season was defined as 3 months from 1 September in all 4 years. A telephone survey was carried out to check the vaccination rate in the Elderly Health Centre cohort.

This study obtained ethical approval from the Joint Institutional Review Board of The University of Hong Kong and Hospital Authority West Cluster, and the Ethics Committee of the Department of Health, Hong Kong.

Results

In a telephone survey from October 2006 to January 2007, of 286 randomly selected Elderly Health Centre enrolees, 207 (72%) responded; 6% reported an influenza vaccination in 2000 to 2002, and 36% in 2003 to 2005. There were 66 820 enrolees at the Elderly Health Centres between July 1998 and December 2001. After excluding 2630 living in institutions, 742 who had died before the start of 2001 or within one year of enrolling, and 145 with no date of death, 63 105 remained. Of these, 17 324 were admitted to hospital and 1582 died in 2001/2; 60 393 survived to the start of 2004, of whom 19 489 were admitted to hospital and 2546 died in 2004/5.

Overall, adjusted admissions for any cause were lower in the 2 years after SARS, with fewer admissions for injury and poisoning (Table), but not pneumonia or respiratory disease. Mortality was similar in both periods, including for injury and poisoning. In the younger age-group, admission was lower for cardiovascular and cardiorespiratory diseases. There was no evidence of different patterns for cardiorespiratory admissions or all-cause mortality by smoking status, self-rated health, overall health status or CSSA status either for all ages or for the younger age-group.

Comparing cardiorespiratory admissions and all-cause mortality by age-group for each possible pair of years in the high and low influenza seasons, there was no discernable pattern of reductions in the high influenza season which were not evident in the low influenza season (Fig).

Discussion

After the SARS outbreak in 2003, the influenza vaccination

Table. Adjusted relative risks* (incident rate ratios) for numbers of admission and ortality in 2004/5 (post-SARS) versus in 2001/2 (pre-SARS) by cause and age-group in the Elderly Health Centre Cohort

Variable	Incident rate ratio (95% CI)		
	All ages	65-74 years	≥75 years
No. of admission (ICD9 CM codes)			
Cancer (140-239)	1.02 (0.88-1.18)	1.03 (0.82-1.28)	1.00 (0.82-1.22)
Cardiovascular (390-459)	0.94 (0.88-1.01)	0.88 (0.78-0.97)	1.01 (0.91-1.11)
Respiratory (11 & 460-519)	0.96 (0.88-1.05)	0.91 (0.78-1.06)	1.01 (0.90-1.13)
Pneumonia (480-487)	3.10 (1.87-5.13)	2.49 (1.17-5.31)	3.54 (1.75-7.16)
Cardiorespiratory	0.95 (0.90-1.01)	0.89 (0.82-0.99)	1.01 (0.93-1.10)
Injury & poisoning (800-999 or E codes)	0.83 (0.78-0.89)	0.81 (0.71-0.92)	0.86 (0.77-0.96)
All other	0.88 (0.85-0.92)	0.84 (0.80-0.89)	0.93 (0.88-0.98)
All	0.91 (0.88-0.95)	0.87 (0.83-0.92)	0.96 (0.92-1.01)
Mortality (ICD10 codes)			
Cancer (C00 to D49)	1.04 (0.90-1.19)	1.06 (0.83-1.34)	1.02 (0.85-1.22)
Cardiovascular (I00-I99)	0.97 (0.82-1.15)	0.72 (0.56-0.93)	1.08 (0.86-1.34)
Respiratory (J00-J99 except J969 and A162, A165, A168, A169)	1.40 (0.98-2.00)	1.08 (0.62-1.87)	1.50 (0.99-2.27)
Pneumonia (J09-J18)	1.63 (0.92-2.88)	1.68 (0.35-8.14)	1.61 (1.52-1.71)
Cardiorespiratory	1.11 (0.95-1.29)	0.83 (0.65-1.05)	1.22 (0.99-1.50)
Injury & poisoning (S00-T98)	1.06 (0.58-1.94)	1.22 (0.36-4.19)	1.03 (0.50-2.14)
All other	1.11 (0.84-1.46)	1.01 (0.61-1.70)	1.14 (0.82-1.58)
All	1.07 (0.97-1.18)	0.97 (0.83-1.14)	1.12 (0.99-1.26)

* Model adjusted for sex, age, education level, and smoking status
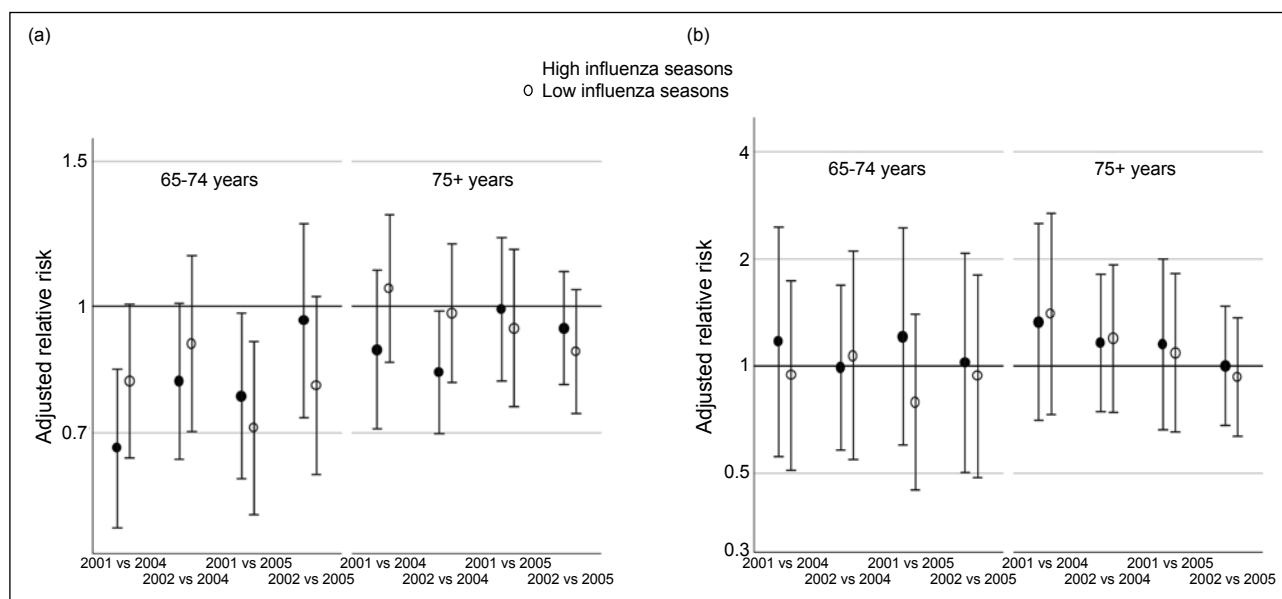
Fig. Adjusted relative risks (incident rate ratios) for (a) cardiorespiratory admission and (b) all-cause mortality in the high and low influenza seasons by age-group for each possible of years

rate in community-dwelling older people increased from low levels to over 35%. Influenza activity in Hong Kong peaked early in the year and dipped in the autumn. In the Elderly Health Centre cohort, there was an 11% reduction in cardiorespiratory hospitalisation in older people aged 65 to 74 years, and possibly a 28% reduction in cardiovascular mortality in the same age-group in the 2 years (2004/5), with more widespread influenza vaccination. These findings are consistent with a review suggesting that influenza vaccination reduces hospitalisation for respiratory diseases by 22%, for cardiac diseases by 24%, and for all-cause mortality by 48%.[2] Nonetheless, in our study, there was no change in all-cause mortality, with a plausible no change in injury and poisoning mortality. An alternative interpretation is that the reduction in hospital use is not causally related to influenza vaccination. First, there was also a similar reduction in hospitalisation for causes other than cancer, respiratory disease, and cardiovascular disease and a larger reduction for injury and poisoning. Moreover, reductions were not specific to the high influenza seasons. Second, following the SARS outbreak more attention in Hong Kong has been focused on preventing the spread of infections, which could lead to lower disease transmission. Third, an 11% reduction in cardiorespiratory hospitalisation is equivalent to an absolute decrease of 566 hospitalisation per 100 272 person years, whereas the number of cardiorespiratory hospitalisation due to influenza is estimated at 723 per 100 000 person years.[5] Reducing the number of cardiorespiratory hospitalisation due to influenza by 78% when vaccinating 36% of the cohort seems unlikely. Nevertheless, the possibility of a smaller beneficial effect of vaccination on hospitalisation cannot be ruled out. In addition, we were not able to consider less serious illnesses not requiring hospitalisation, which may make a difference to an older person's quality of life.

Limitations

First, this study was limited by lack of information on individual vaccination records, which are not centrally accessible. Those unvaccinated in the first period were not unvaccinated by self-selection, but by a policy decision, thus removing some of the potential volunteer bias. It is possible that mainly 'healthy users' who were not susceptible to the complications of influenza received vaccination, although vaccination was targeted at the needy and those with chronic diseases and there was no evidence of different effects by health status. Second, the study only considered a limited number of influenza seasons, which are not directly comparable. Nonetheless, the seasons in 2002 and 2004 appear similar, and a comparison of these influenza seasons found little difference in hospitalisation or mortality. The influenza strains in circulation have not changed greatly in several years,[3] so many older people may have already acquired natural immunity. Third, hospitalisation and death rates for pneumonia were higher post-SARS, which could represent an increase in pneumonia or more likely greater vigilance and more complete ascertainment of pneumonia. Finally, the model may be mis-specified, however, hospitalisation for cancer was similar in both periods, as were deaths from injury and poisoning.

Conclusions

Influenza vaccination may be beneficial and may protect older people from morbidity and mortality, but it is unlikely that influenza vaccination in Hong Kong would reduce all-cause mortality in the influenza season by half, or cardiorespiratory hospitalisation by a quarter. To what extent influenza vaccination protects older people in sub-tropical regions from serious morbidity and mortality needs

to be confirmed in appropriately designed studies, so that scarce health care resources can be used effectively.

Acknowledgements

References

1. Viboud C, Alonso WJ, Simonsen L. Influenza in tropical regions. PLoS Med 2006;3:e89.
2. Jefferson T, Rivetti D, Rivetti A, Rudin M, Di Pietrantonj C, Demicheli V. Efficacy and effectiveness of influenza vaccines in elderly people: a systematic review. Lancet 2005;366:1165-74.
3. Simonsen L, Reichert TA, Viboud C, Blackwelder WC, Taylor RJ, Miller MA. Impact of influenza vaccination on seasonal mortality in the US elderly population. Arch Intern Med 2005;165:265-72.
4. Cowling BJ, Wong IO, Ho LM, Riley S, Leung GM. Methods for monitoring influenza surveillance data. Int J Epidemiol 2006;35:1314-21.
5. Wong CM, Yang L, Chan KP, et al. Influenza-associated hospitalization in a subtropical city. PLoS Med 2006;3:e121.

Hong Kong team:
CM Wong 黃浙明
JSM Peiris 裴偉士
L Yang 楊　琳
KP Chan 陳敬斌
TQ Thach 石國順
HK Lai 黎克勤
WWL Lim 林薇玲
AJ Hedley 賀達理
Guangzhou team:
J He 何劍峰
P Chen 陳平雁
C Ou 歐春泉
A Deng 鄧愛萍
X Zhang 張　欣
D Zhou 周端華
Singapore team:
S Ma 馬時樂
A Chow 周莉萍

Effect of influenza on cardiorespiratory and all-cause mortality in Hong Kong, Singapore and Guangzhou

· ·

Key Messages

1. Using a common modelling approach, mortality attributable to influenza was higher in the two subtropical cities Guangzhou and Hong Kong than in the tropical city Singapore.
2. The virus activity appeared more synchronised in subtropical cities, whereas seasonality of influenza tended to be less marked in the tropical city.
3. High temperature was associated with increased mortality after influenza infection in Hong Kong, whereas relative humidity was an effect modifier for influenza in Guangzhou. No effect modification was found for Singapore.
4. Seasonal and environmental factors probably play a more important role than socioeconomic factors in regulating seasonality and disease burden of influenza. Further studies are needed in identifying the mechanism behind the regulatory role of environmental factors.

Li Ka Shing Faculty of Medicine, The University of Hong Kong:
Department of Community Medicine and School of Public Health
CM Wong, L Yang, KP Chan, TQ Thach, HK Lai, AJ Hedley
Department of Microbiology
JSM Peiris
Public Health Laboratory Service Branch, Department of Health, Hong Kong
WWL Lim
Guangdong Provincial Center for Disease Control and Prevention
J He, A Deng, X Zhang, D Zhou
Department of Biostatistics, School of Public Health and Tropical Medicine, South Medical University, Guangzhou
P Chen, C Ou
Epidemiology and Disease Control Division, Ministry of Health, Singapore
S Ma
Communicable Disease Centre, Tan Tock Seng Hospital, Singapore
A Chow

Introduction

Influenza has been associated with considerable mortality in temperate regions. The disease burden of influenza in subtropical and tropical regions are less known. Influenza viruses may exhibit various levels of virulence each year as a result of frequent antigenic drifts. There is disparity between geographical areas even in the same influenza season. Socioeconomic factors and circulating virus strains could play a role in determining the severity of influenza epidemics.[1] Several large-scale phylogenetic studies have postulated that novel influenza viruses first emerge in the East and Southeast Asia. It is therefore important to understand the seasonality and disease burden of influenza in these regions.

The same modelling methods were applied to three metropolitan cities: Guangzhou, Hong Kong, and Singapore. All have standardised influenza surveillance networks. Guangzhou and Hong Kong are subtropical cities, whereas Singapore is a tropical city. The similarity and differences between these cities in terms of socioeconomic status and environmental factors enable exploration of factors in terms of the disease burden of influenza.

Methods

This study was conducted from 1 July 2006 to 31 December 2008. All three cities have similarly designed surveillance networks for influenza, in which specimens are collected from both outpatients and inpatients throughout the year. Weekly data of virology surveillance, meteorology, and mortality from each city were obtained and aggregated. To reduce the bias introduced by unequal numbers of specimens taken each week, proportions of specimens positive for influenza were used as measures for influenza virus activity. Five causes of death were associated with influenza: cardiorespiratory diseases (CRD), pneumonia and influenza (P&I), chronic obstructive pulmonary diseases (COPD), ischaemic heart diseases (IHD), and all-cause deaths.

Poisson regression models were used to assess the percentage of excess mortality associated with increased influenza activity in the population.[2] This modelling method is well suited to the subtropics and tropics where influenza can be active throughout the year and usually without a clear pattern of epidemics. Briefly, weekly mortality, with the weekly proportions of specimens positive for each influenza type/subtype (named as virus activity) was used. Yearly dummy variables and the product terms between yearly dummies and virus activity were used as independent variables. Several confounders, including long-term trends and seasonal variations in mortality, weekly temperature and humidity, were simultaneously added into the models. The effects of influenza were estimated by the excess rates of mortality, which was calculated as the difference between the number of observed deaths and the estimated number under the assumption of no virus activity, and then divided by the total number of observed deaths.

To explore whether the regional heterogeneity of influenza-associated mortality was due to effect modification of temperature, the whole study period

was divided into high, medium, and low temperature periods, with the first and third quartiles of weekly average temperatures as the cut-off points. Interaction models for all-cause, CRD and P&I mortality of each city were built, in which the product terms of virus activity and dummy variables for three temperature periods were added together with previously described confounders. The significance of effect modification by temperature was evaluated by the likelihood ratio tests between models with and without interaction terms. Based on the interaction models, the percentages of excess deaths among total observed deaths associated with each measure of observed virus activity for the high, medium, and low temperature periods were computed. Similar analyses were repeated for weekly average humidity, which was also stratified into the high, medium, and low humidity periods, with the first and third quartiles as cut-off points.

Results

Among the three cities, Singapore is hottest and most humid and its population is the youngest. The overall mortality rate of Guangzhou was highest. The average proportions of positive influenza isolates in all specimens, known as influenza virus activity, were lowest in Singapore. The dominant virus types/subtypes were consistent among three cities: A/H3N2 was dominant in year 2004 and 2005, whereas A/H1N1 and B were more prevalent in 2006.

During 2004-2006 for all-age groups in all three cities, influenza was significantly associated with all-cause mortality as well as mortality with underlying causes of CRD, P&I, COPD, and IHD ($P<0.05$), with the exceptions of P&I in Guangzhou, COPD in Singapore, and IHD in Hong Kong (Table 1). Among the three cities, Hong Kong had the highest excess mortality with underlying causes of P&I, COPD, and all causes, whereas influenza in Guangzhou was associated with most deaths caused by CRD and IHD. For the elderly aged ≥65 years, Guangzhou had the highest excess mortality for both all-cause and CRD mortality, and Singapore had the lowest rate. The year 2005 entailed the greatest disease burden of influenza for all three

Table 1. The annual excess   ortality per 100 000 population associated with influenza in all-age groups

Cause of death	Annual excess mortality (95% CI)		
	Guangzhou	Hong Kong	Singapore
All causes			
2004	10.7 (-3.2, 25.2)	0.0 (-12.7, 12.7)	17.0 (7.2, 26.8)
2005	21.5 (-2.5, 43.7)	28.1 (17.1, 39.2)	5.7 (-3.4, 14.8)
2006	4.8 (-9.6, 18.0)	13.2 (-2.1, 27.4)	3.3 (-4.8, 1 .1)
Overall	12.4 (1.2, 23.0)	13.9 (6.4, 20.9)	8.7 (3.0, 13.9)
Cardiorespiratory diseases			
2004	9.5 (-1.4, 20.5)	2.1 (-5.9, 10.1)	7.5 (0.2, 14.8)
2005	18.8 (0.0, 36.3)	18.6 (11.6, 25.3)	5.6 (-1.2, 12.0)
2006	5.3 (-5.7, 15.4)	6.3 (-3.7, 15.5)	3.6 (-2.1, 9.3)
Overall	11.2 (2.4, 19.6)	9.1 (4.3, 13.6)	5.6 (1.6, 9.4)
Pneumonia and influenza			
2004	0.3 (-0.8, 1.4)	1.2 (-2.3, 4.4)	3.1 (-0.7, 6.7)
2005	1.4 (-0.5, 3.1)	8.8 (6.0, 1 .6)	3.8 (0.3, 7.2)
2006	0.2 (-1.0, 1.3)	4.2 (0.0, 8.0)	1.8 (-1.3, 4.9)
Overall	0.6 (-0.3, 1.5)	4.7 (2.7, 6.7)	2.9 (0.8, 4.9)
Chronic obstructive pulmonary diseases			
2004	0.9 (-2.1, 3.7)	0.5 (-1.8, 2.7)	-1.3 (-3.6, 0.7)
2005	4.7 (0.1, 8.9)	5.4 (3.7, 7.0)	0.2 (-1.7, 1.9)
2006	1.2 (-1.5, 3.6)	1.5 (-0.9, 3.8)	-0.2 (-2.2, 1.1)
Overall	2.3 (0.0, 4.4)	2.5 (1.2, 3.7)	-0.5 (-1.7, 0.5)
Ischaemic heart diseases			
2004	2.2 (-0.9, 5.1)	2.1 (-1.1, 5.2)	2.9 (-1.5, 7.0)
2005	6.3 (1.3, 10.8)	2.3 (-0.2, 4.7)	3.9 (-0.2, 7.6)
2006	1.8 (-1.3, 4.6)	0.7 (-3.2, 4.3)	1.0 (-2.5, 4.3)
Overall	3.4 (1.0, 5.6)	1.7 (-0.2, 3.5)	2.6 (0.2, 4.7)

Table 2. The annual excess   ortality per 100 000 population associated with influenza in the ≥65-year-old age group

Cause of death	Annual excess mortality (95% CI)		
	Guangzhou	Hong Kong	Singapore
All causes			
2004	108.9 (-14.8, 237.5)	10.3 (-86.0, 1 0.0)	202.3 (79.5, 325.1)
2005	212.5 (-4.9, 415.2)	211.4 (129.0, 293.8)	74.0 (-35.2, 183.3)
2006	60.1 (-69.4, 180.4)	73.7 (-40.2, 184.4)	13.5 (-81.0, 1 .4)
Overall	130.6 (24.2, 227.4)	100.3 (44.9, 155.6)	94.5 (28.0, 161.0)
Cardiorespiratory diseases			
2004	100.3 (-3.2, 207.1)	27.9 (-36.6, 92.4)	91.4 (-4.4, 189.4)
2005	185.7 (6.3, 349.5)	148.1 (95.1, 201.1)	74.1 (-14.8, 156.8)
2006	58.8 (-44.8, 154.0)	46.9 (-28.5, 1 7.2)	15.9 (-57.6, 87.3)
Overall	116.3 (30.6, 195.9)	75.2 (38.5, 111.9)	58.5 (8.4, 110.8)
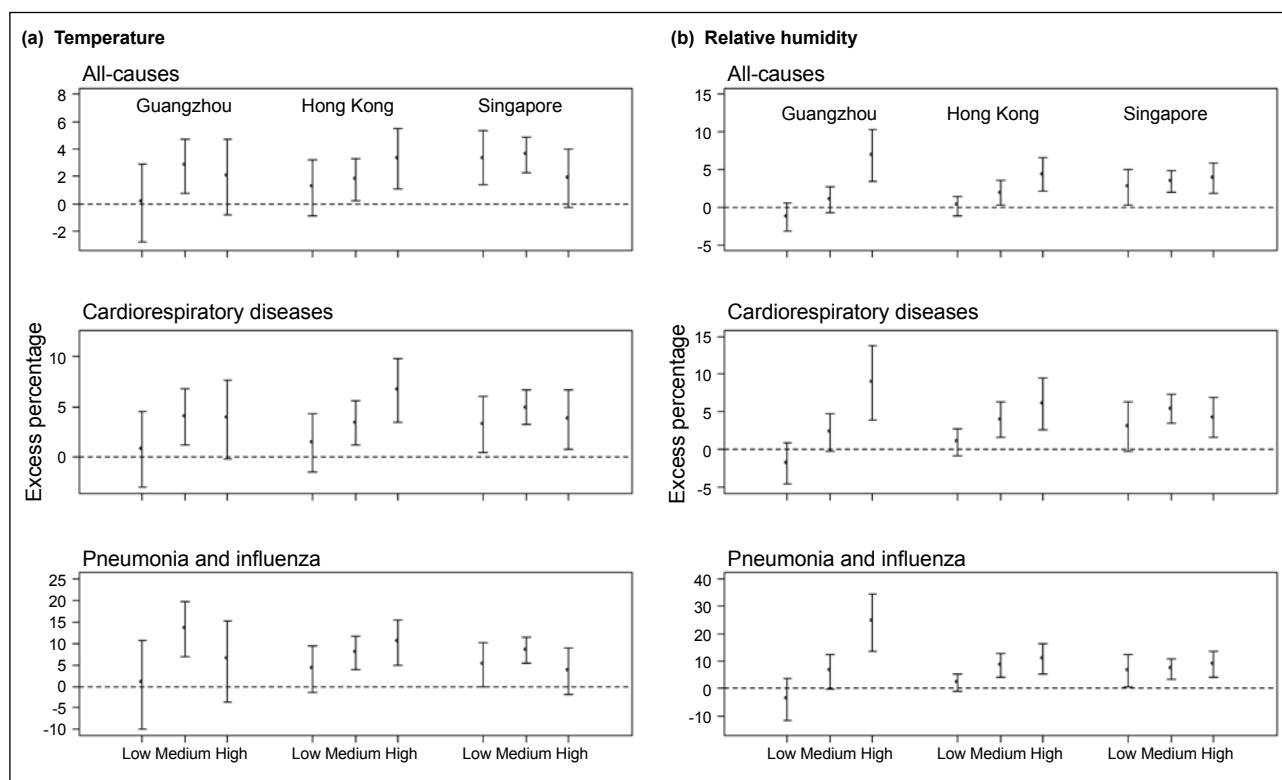
Fig. Excess percentages associated with influenza during the low, medium, and high periods stratified by weekly average (a) temperature and (b) relative humidity, for Guangzhou, Hong Kong, and Singapore

cities. The year entailed the lowest disease burden was 2006 for Guangzhou and Singapore, and 2004 for Hong Kong (Table 2).

Likelihood ratio tests between the interaction and main effect models showed that the difference between temperature periods was likely due to chance (P>0.05), except the CRD mortality in Hong Kong (P=0.006, Fig). The highest excess percentages were in medium temperature periods in both Guangzhou and Singapore, but were in high temperature periods in Hong Kong. The interaction of relative humidity and influenza was significant in the all-cause mortality in Hong Kong (P=0.006) and in all-cause and CRD mortality (P<0.001) in Guangzhou. Influenza accounted for more deaths during the high humidity periods in Guangzhou and Hong Kong, whereas influenza effects were similar across humidity strata in Singapore.

Discussion

This study systematically compared the influenza-associated disease burdens in three metropolitan cities in Asia. The surveillance networks for influenza in Guangzhou, Hong Kong, and Singapore were constructed under the World Health Organization Global Influenza Surveillance Network, which estimate disease burdens using a standardised procedure for comparison. Similar Poisson regression models were adopted to assess age- and disease-specific excess mortality associated with influenza,

allowing for flexible adjustment of seasonal confounding factors. This model has been widely used in other disease burden studies and recommended for subtropical and tropical regions with unpredictable influenza seasonality.[3] However, this approach requires long-standing year-round surveillance that has not yet been established in many subtropical and tropical regions. Nevertheless, our study provides a good example for the future disease burden studies and for the development of more surveillance centres.

Influenza-associated mortality rates were comparable in Hong Kong and Singapore. Singapore even had a higher excess mortality for the elderly.[2,4] However, slightly different models were used and different study periods were covered. In this study, the estimates of tropical Singapore remained lower than those of the other two subtropical cities for all the disease categories under study. Given the similar socioeconomic development levels in Hong Kong and Singapore, environmental and geographical factors may affect the severity of influenza to a greater extent than socioeconomic factors. The close geographical location of Guangzhou and Hong Kong may result in similar circulating influenza strains as well as pre-existing immunity in the population, but this hypothesis is not supported by our subtype-specific estimates, as a great heterogeneity could still be observed between the two cities. In future, a large-scale phylogenetic analysis for the circulating strains in these cities may provide information about this hypothesis.

Cold temperature and dry air facilitate the transmission of influenza virus and prolong their survival in the air.[5] Most studies were conducted at temperatures <30°C and relative humidity <80%. In our study, there was a significant linear trend for influenza-associated risks as temperature increased in Hong Kong, particularly for CRD deaths. This indicates that cold temperature may not increase the chances of deaths subsequent to influenza infections, although the possibility of increased transmission under low temperature could not be ruled out by our study. Such an effect modification by temperature may be due to widespread use of air conditioners in Hong Kong. The great difference between indoor and outdoor temperature could weaken the host immunity response against infection and the closed circulation of indoor air could facilitate virus transmission. Apparently in Guangzhou, humidity rather than temperature is the modifier for the effects of influenza, which exhibited a linear trend across three humidity strata for all-cause, CRD and P&I deaths. This could be explained by the higher annual variation of humidity in Guangzhou compared to the other two cities. Similarly, the absence of modification by temperature or humidity on influenza effects in Singapore could be due to its low variation of temperature and humidity throughout the year.

Our findings on regional heterogeneity of influenza disease burden and potential modification of environmental factors on influenza effects could shed more light on mechanisms of influenza seasonality and suggests a need to refine surveillance and control strategies against influenza specific to each region. In future, a multinational study involving more temperate and tropical, as well as developed and developing countries could provide more information about mechanisms and effect modifiers for the severity of influenza epidemics or pandemics.

Acknowledgements

References

1. Viboud C, Tam T, Fleming D, Miller MA, Simonsen L. 1951 influenza epidemic, England and Wales, Canada, and the United States. Emerg Infect Dis 2006;12:661-8.
2. Wong CM, Chan KP, Hedley AJ, Peiris JS. Influenza-associated mortality in Hong Kong. Clin Infect Dis 2004;39:1611-7.
3. World Health Organization. A practical guide for designing and conducting influenza disease burden studies. 2008.
4. Chow A, Ma S, Ling AE, Chew SK. Influenza-associated deaths in tropical Singapore. Emerg Infect Dis 2006;12:114-21.
5. Lowen AC, Mubareka S, Steel J, Palese P. Influenza virus transmission is dependent on relative humidity and temperature. PLoS Pathog 2007;3:1470-6.

DCW Lee 李振威
AHY Law 羅興怡
K Hui 許珮茵
AHM Tam 譚浩文
JSM Peiris 裴偉仕
ASY Lau 劉錫賢

Interferon dysregulation and virus-induced cell death in avian influenza H5N1 virus infectionsz

Key Messages

1. Hyper-induction of cytokines and chemokines was found in human blood macrophages infected with the avian influenza H5N1 and H9N2/G1 viruses, as compared to those infected with human influenza H1N1 virus.
2. IRF3 played a significant role in the hyperinduction of cytokines including IFN-β, IFN-λ1, IFN-α subtypes, MCP-1, and TNF-α, and also played a part in subsequent cytokine-induced cell signalling cascades.
3. Compared with H1N1 viruses, avian influenza viruses including H5N1/97 and its precursors triggered a caspase-mediated but delayed apoptotic response in human macrophages.
4. Therapies that can minimise immunopathology-associated dysregulation of innate immunity without impairing effective host defence may be valuable adjuncts to antiviral therapy.

Li Ka Shing Faculty of Medicine, The University of Hong Kong:
Department of Paediatrics and Adolescent Medicine
DCW Lee, AHY Law, AHM Tam, ASY Lau
Department of Microbiology
K Hui, JSM Peiris

RFCID project number: 05050112

Principal applicant and corresponding author:
Prof Allan Sik-yin Lau
Department of Paediatrics and Adolescent Medicine, The University of Hong Kong, 1/F New Clinical Building, Queen Mary Hospital, Pokfulam Road, Hong Kong SAR, China
Tel: (852) 2255 4269
Fax: (852) 2855 1523
Email: asylau@hku.hk

Introduction

A novel influenza A H1N1 virus of swine origin caused an influenza pandemic in 2009,[1] but avian influenza H5N1 virus remains the major concern to humans. Since the first documented cases of avian influenza H5N1/97 virus in Hong Kong, these viruses have continued to evolve and cause outbreaks in poultry in European and Asian countries.[2] Sporadic cases of human infections have high mortality rates of >60%.[1] Understanding its pathogenesis enhances the development of novel therapy.

Influenza A viruses are known to replicate in epithelial cells and leukocytes, resulting in induction of cytokines and chemokines, including TNF-α, IL-1β, IL-6, IP-10, RANTES, MCP-1, and interferons (IFN-α and -β). Using our H5N1/97-macrophage model, H5N1/97 induced dramatically higher levels of cytokine expression, compared to those infected with 'seasonal flu' human H1N1 or H3N2 viruses. Subsequently, the TNF induction and its cytotoxicity were mediated, at least in part, by mitogen-activated protein kinases, including p38 and ERK.[3]

We further investigated the underlying mechanisms of interferon dysregulation and virus-induced cell death in influenza-infected cells by examining the activation of different types of transcription factors. The expressions of IFN- β, IFN-λ1 and TNF-α were regulated by IRF-3 following virus infections. Moreover, a delayed onset of caspase-mediated apoptotic pathways was found in H5N1-infected human macrophages, compared to those infected by non-avian viruses. These findings may be useful for the design of novel immunotherapeutic regimens to abrogate or lessen the cytokine dysregulation in those highly pathogenic avian viruses.

Methods

This study was conducted from 1 October 2006 to 30 September 2008. Peripheral blood monocytes were isolated from buffy coats of healthy donors (from the Hong Kong Red Cross Blood Transfusion Service) by Ficoll-Paque (Pharmacia Biotech) density gradient centrifugation and purified by adherence.[3] The purity of the monocyte preparations was examined by immunostaining with anti-CD14 antibodies (BD Biosciences). The cells were allowed to differentiate for 14 days in RPMI 1640 medium supplemented with 5% heat-inactivated autologous plasma. Macrophages were seeded onto 24-well (1.5×10^5 cells/well) tissue culture plates for studies of mRNA expression. Differentiated macrophages were incubated in serum-free macrophage SFM medium (GIBCO BRL) supplemented with 0.6 μg/mL penicillin and 60 μg/mL streptomycin (Sigma-Aldrich) one day before virus challenge.

H5N1 influenza viruses A/HK/483/97 (H5N1/97) and A/Vietnam/3212/04 (H5N1/04) isolated from H5N1-infected patients were cultured in Madin Darby canine kidney cells. Precursors of H5N1/97, A/Quail/Hong Kong/G1/97 (H9N2/G1) virus, and seasonal human influenza H1N1 virus A/HK/54/98 (H1N1) were

isolated from other infected patients. These viruses were then purified by pre-adsorption to and elution from Turkey red blood cells.[3] Virus stock was aliquoted and stored at -80ºC until use.

Differentiated macrophages were infected at a multiplicity of infection of two for 30 to 45 minutes. Then, the virus inoculum was removed and the cells were washed once and incubated in macrophage SFM medium supplemented with 0.6 μg/mL penicillin, 60 μg/mL streptomycin, and 2 μg/mL N-p-tosyl-L-phenylalaninechloromethyl ketone-treated trypsin (Sigma-Aldrich). The culture supernatant was collected for cytokine analysis and the total cellular RNA was extracted for gene expression analysis at indicated times. Duplicate wells of monolayer cells were fixed and analysed by immunofluorescent staining for influenza virus-specific nucleoprotein (DAKO Imagen) at 8 hours post-infection.

DNase-treated total RNA, isolated by RNeasy Mini Kit (Qiagen), was reverse-transcribed by using poly(dT) primers and Superscript III reverse transcriptase (Invitrogen) and quantified by real-time PCR analysis with a LightCycler (Roche Diagnostics). The methods used for quantifying cytokine and β-actin mRNA have been described.[4]

Macrophages on coverslips were infected with influenza virus for 3 hours. Cells were fixed with 4% paraformaldehyde and permeabilised with 0.2% Triton X-100 dissolved in PBS. Cells were washed with PBS, stained with anti-IRF3 antibodies, washed and stained with fluorescein-conjugated anti-rabbit Ig (ZyMed). Nuclei of the cells were counter-stained with 1 μg/mL of DAPI (Sigma-Aldrich) and mounted in 50% glycerol in PBS.

Whole cell extracts were prepared by lysing macrophages with cold whole cell lysis buffer (50 mM KCl, 1% NP-40, 25 mM HEPES [pH 7.4], 1 mM DTT, protease inhibitor cocktail [Roche Diagnostics] and phosphatase inhibitor cocktail [Calbiochem]) on ice for 10 minutes. The cell lysates were collected with a cell scraper and the whole cell extract was harvested by centrifugation at 13 000 rpm for 10 minutes at 4ºC. The protein content was determined

with a Bio-Rad Protein Assay (Bio-Rad Laboratories) using BSA as a standard.

Thirty micrograms of whole cell lysate or 15 μg of cytoplasmic protein was heat denatured in a sample buffer (62.5 mM Tris [pH 6.8], 35% glycerol, 2% SDS, 5% 2-mercaptoethanol, 0.05% bromophenol blue), separated by using 8% SDS-PAGE and transferred to polyvinylidene difluoride or nitrocellulose membranes. The membranes were immersed with 5% skim milk/PBS for 1.5 hours and immunoblotted with primary antibodies. Anti-actin antibodies were used as loading controls for the cytoplasmic fraction. The immunoblots were then incubated with HRP-coupled goat anti-rabbit or anti-mouse IgG antibodies, and the signals were visualised by ECL plus solution (GE Healthcare).

Results

A hyper-induction of IFN-β and IFN-α was found in human blood macrophages infected with the avian influenza H5N1 and H9N2/G1 viruses, as compared with those infected with human influenza H1N1 virus. There was a differential induction of IFN-α subtypes including IFNα1, 2 and 8 in H9N2/G1-infected cells by using genechip analysis, as compared with those induced by H1N1 (Table). The results were validated by Q-PCR and ELISA assay (data not shown).

There was hyperinduction of cytokines and chemokines, including IFN-β, IFN-λ1, TNF-α, IP-10, MCP-1, MIP-1α, and RANTES in H5N1-infected macrophages.[4] To investigate the mechanisms of cytokine induction, IRF3 activation in virus-infected macrophages was examined by immunofluorescent staining. A differential IRF3 activation was found in macrophages infected with H5N1 viruses, compared to those infected with H1N1 virus (Fig 1). By using the IRF3-specific siRNA oligos, the mRNA levels of IFN-β and IFN-λ1 inducible by the H5N1 virus were abrogated.[4] The IRF3 was the key transcription factor for IFN gene regulation. However, the up-regulation of TNF-α in H5N1-infected macrophages was moderately suppressed by IRF3 siRNA, indicating that IRF3 only contributed, in

Table. Differential induction of IFN-α subtypes in influenza virus infections

IFN-α subtype	3 hours post-infection			8 hours post-infection		
	Mock	H1N1	H9N2	Mock	H1N1	H9N2
IFN-α		16.11	214.40		37.25	175.9
IFN-α 2		2.53	25.74		2.78	18.56
IFN-α 4		1.40	10.14		1.30	3.67
IFN-α 7		1.51	8.11		2.12	5.72
IFN-α 8		1.93	25.03		2.97	26.35
IFN-α 10		1.30	2.64		1.71	5.39
IFN-α 13		5.80	70.92		5.46	25.55
IFN-α 14		1.76	13.12		2.31	7.04
IFN-α 16		1.36	9.49		2.31	7.79
IFN-α 17		1.14	2.99		1.22	2.65
IFN-α 21		1.39	3.96		2.18	6.07
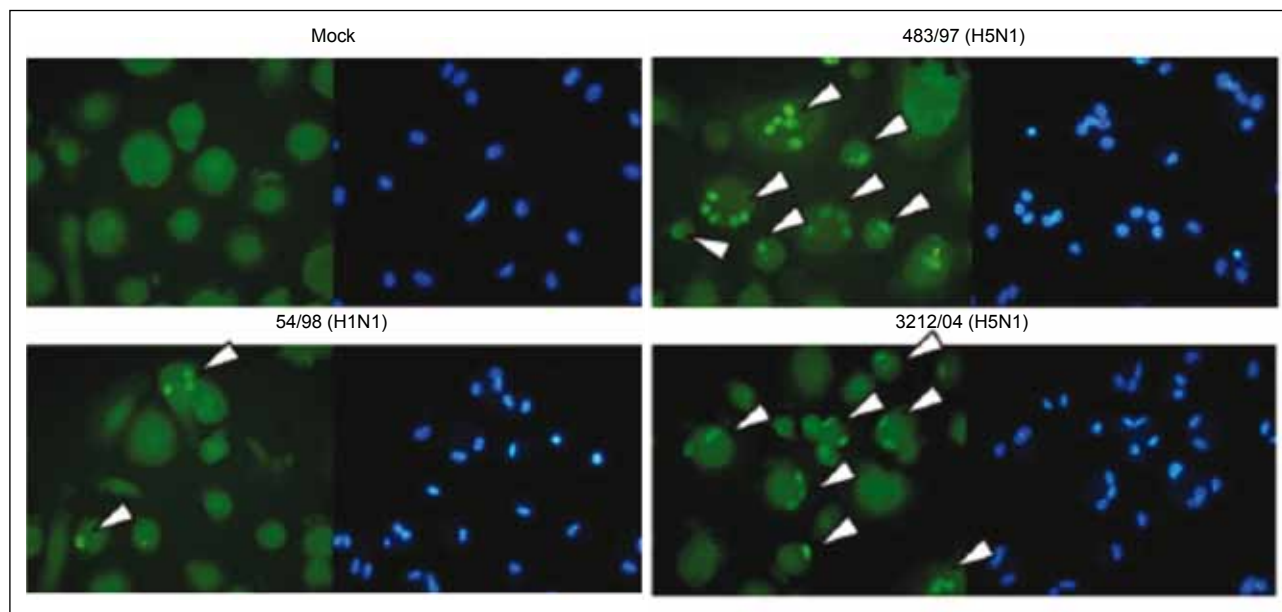
Fig 1. H5N1 viruses differentially activate IRF3 translocation as compared to H1N1 virus
Differentiated primary human macrophages were infected with 54/98 (H1N1), 483/97 (H5N1), or 3212/04 (H5N1) at a multiplicity of infection of two. Mock infected cells served as controls. Immunofluorescence staining assay of IRF3 translocation. At 3 hours post-infection, the cells were fixed with 4% paraformaldehyde. Permeabilised cells were stained with anti-IRF3 Ab and FITC-conjugated secondary Ab. Cell nuclei were counter-stained with DAPI. Cells with IRF3 translocation were indicated with arrowheads. (Figures were adopted from J Immunol 2009;182:1088-98 with permission, approval pending)
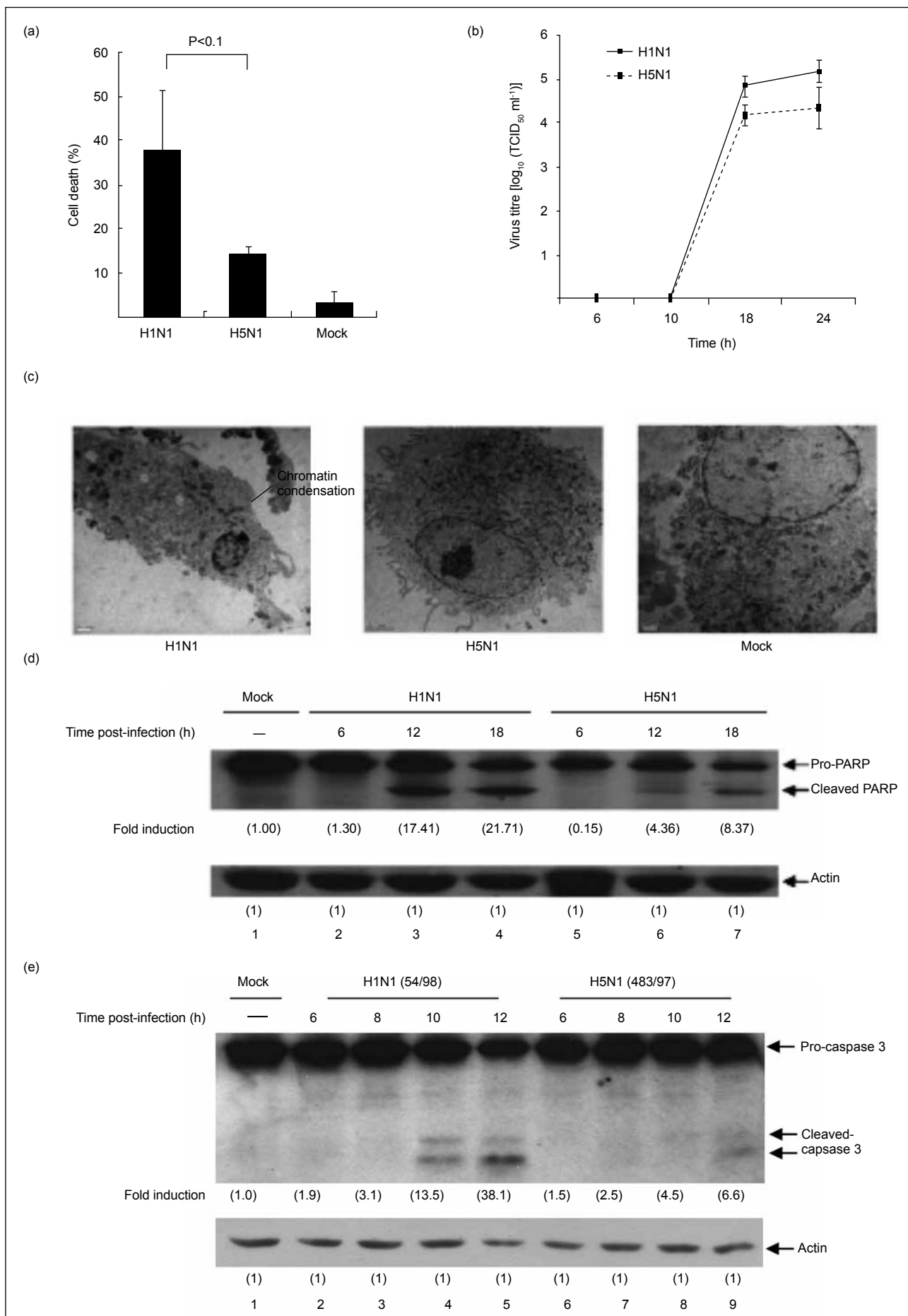
part, to the H5N1-induced TNF-α expression. Other H5N1-induced cytokines including IP-10, RANTES, MCP-1, and MIP-1α were inhibited by the IRF3-specific siRNA.[4] As the expression of these cytokines may involve de novo protein synthesis, the detailed regulatory mechanism needs to be investigated. Interestingly, IRF3 showed similar regulatory roles on cytokine expression induced by H1N1 virus, although the potency of H1N1 was less than that of H5N1 virus (data not shown). Additional results delineating the role of IRF-3 have been reported.[4]
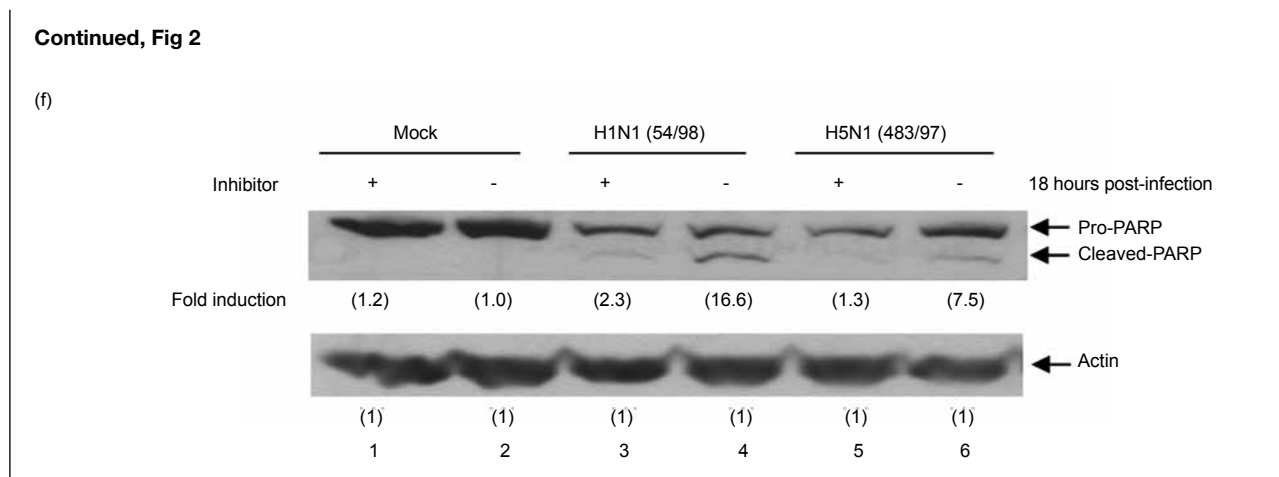
In addition to the mechanism of cytokine induction, the onset of cell death in human macrophages infected with the H5N1/97 virus and its precursors was delayed. Primary macrophages were mock-treated or infected with H5N1/97 or H1N1 influenza viruses at a multiplicity of infection of two for 30 minutes and harvested at indicated time points for analysis. At 18 hours post-infection, infected cells were examined by staining with 4,6-diamidine-2-phenylindole dihydrochloride (DAPI) and cell death was determined by nuclear condensation or nuclear fragmentation. Less dead cells was found after H5N1/97 than H1N1 virus infection (Fig. 2a). There was no significant difference of viral replication in the macrophages infected by H1N1 or H5N1/97 (Fig. 2b). Using transmission electron microscopy, the cellular morphology of H5N1/97-infected macrophages was comparable to that of the mock-treated cells at 12 hours post-infection (Fig 2c). In contrast, the characteristics of apoptotic cells including nuclear condensation and chromatin adherence to nuclear membrane were noted in the H1N1-infected cells (Fig 2c). Our results demonstrated

a differential onset of cell death in macrophages infected with the H5N1/97 compared to those infected with the H1N1 virus.

The activity of caspase-activated poly [ADP-ribose] polymerase (PARP, Pharmingen) was further examined at 6, 12, and 18 hours post-infection, using Western analysis (Fig 2d). Over the time course, the levels of the cleaved-PARP fragment in the H5N1/97-infected cells were lower than those in the H1N1-infected cells (Fig 2d). The activity of caspase 3 was then measured by Western analysis. In contrast to a strongly cleaved caspase 3 fragment found in the H1N1-infected cells at 10 hours, caspase 3 was barely activated in the H5N1/97-infected cells at 12 hours (Fig 2e). By treating virus-infected cells with a specific caspase inhibitor, Z-IETD-FMK, the level of the cleaved-PARP fragment in H5N1/97- or H1N1-infected macrophages was significantly reduced by 82% and 86%, respectively, as compared to the corresponding untreated samples (Fig 2f). Hence, the delayed activation of the caspase cascade in H5N1/97 infected cells appears to determine the differential onset of cell death in H5N1/97 and H1N1 infection. More importantly, the characteristic delayed onset of apoptosis in H5N1/97 infection was also found in its precursor viruses including H9N2/G1, A/Teal/HK/W312/97 (H6N1), and A/Goose/Guangdong/1/96 (H5N1/437.6). All these results have already been reported.[5]

H5N1 virus differentially activates p38 mitogen-activated protein kinases to mediate the hyperinduction of proinflammatory cytokines including TNF-α.[3] H5N1

(a)

(b)

(c)

(d)

	Mock	H1N1			H5N1		
Time post-infection (h)	—	6	12	18	6	12	18
Fold induction	(1.00)	(1.30)	(17.41)	(21.71)	(0.15)	(4.36)	(8.37)
	(1)	(1)	(1)	(1)	(1)	(1)	(1)
	1	2	3	4	5	6	7

(e)

	Mock	H1N1 (54/98)				H5N1 (483/97)			
Time post-infection (h)	—	6	8	10	12	6	8	10	12
Fold induction	(1.0)	(1.9)	(3.1)	(13.5)	(38.1)	(1.5)	(2.5)	(4.5)	(6.6)
	(1)	(1)	(1)	(1)	(1)	(1)	(1)	(1)	(1)
	1	2	3	4	5	6	7	8	9

Continued, Fig 2

(f)

Fig 2. H5N1/97-infected macrophages show less cell death and apoptosis
(a) Primary human blood macrophages (0.5×10^6) were fixed with 4% paraformaldehyde, stained with DAPI at 18 hours post-infection with H5N1 (483/97) or H1N1 (54/98) virus at a multiplicity of infection of two. Values presented as mean±SD of cells from three different donors and statistically analysed by the two-tailed, paired t-test. (b) Primary macrophages (1×10^6) were infected with H1N1 (54/98) or H5N1 (483/97). The culture supernatants were collected at 6, 10, 18, and 24 hours post-infection. The viral titres (TCID50) of the samples were measured by titration in Madin Darby canine kidney cells. The results shown are representative of experiments performed on cells from three different donors. (c) Primary macrophages (2×10^6) were infected with influenza virus H5N1 (483/97) or H1N1 (54/98) at a multiplicity of infection of two. At 12 hours post-infection, the cells were collected for ultrastructural examination by transmission electron microscopy. H1N1-infected macrophages (left), H5N1-infected macrophages (middle), mock-treated macrophages (right) are shown with magnification ×28 000. (d) Primary macrophages (1×10^6) were harvested at 6, 12, and 18 hours post-infection with H5N1 (483/97) or H1N1 (54/98) virus. The activated level of PARP was assayed by Western analysis using a monoclonal anti-PARP antibody. The numbers in the brackets are density values of the activated PARP relative to that of the actin. (e) Delayed activation of caspase 3 in the H5N1-infected human macrophages. Primary macrophages (1×10^6) were harvested at 6, 8, 10, and 12 hours post-infection with H5N1 (483/97) or H1N1 (54/98) virus. The activation of caspase 3 was assayed by Western analysis using polyclonal anti-caspase 3 antibodies. (f) Primary human macrophages (1×10^6) were pretreated with or without 50μM of caspase inhibitor, Z-IETD-FMK, for 1 hour at 37°C and infected with H5N1 (483/97) or H1N1 (54/98) virus, or without infection. The total proteins were harvested at 18 hours post-infection and assayed by Western analysis using anti-PARP antibody. Equal loading of protein samples was determined using anti-actin antibodies. The density of the protein band was determined by using Bio-Rad Quantity One imaging software. The numbers in the brackets are density values of the activated-caspase 3, or activated-PARP relative to that of the actin. (Figures were adopted from J Gen Virol 2007;88:1275-80 with permission, approval pending)

virus differentially activated IRF3 leading to activation of IFNs and chemokines. Moreover, H5N1 and H9N2/G1 viruses triggered a delayed and caspase-mediated apoptotic response in human macrophages as compared with the human influenza viruses. Hence, further investigation of the pathogenic properties of the H5N1 virus including delayed onset of apoptosis and hyperinduction of proinflammatory cytokines may contribute to the understanding of how these novel viruses cause the fatal disease in humans. Furthermore, therapies that minimise immunopathology-associated dysregulation of innate immunity without impairing effective host defence may be valuable adjuncts to antiviral therapy.

Acknowledgements

References

1. World Health Organization avian influenza information. Available at: http://www.who.int/csr/disease/avian_influenza/en/.
2. Guan Y, Shortridge KF, Krauss S, Webster RG. Molecular characterization of H9N2 influenza viruses: were they the donors of the "internal" genes of H5N1 viruses in Hong Kong? Proc Natl Acad Sci USA 1999;96:9363-7.
3. Lee DC, Cheung CY, Law AH, Mok CK, Peiris M, Lau AS. p38 mitogen-activated protein kinase-dependent hyperinduction of tumor necrosis factor alpha expression in response to avian influenza virus H5N1. J Virol 2005;79:10147-54.
4. Hui KP, Lee SM, Cheung CY, et al. Induction of proinflammatory cytokines in primary human macrophages by influenza A virus (H5N1) is selectively regulated by IFN regulatory factor 3 and p38 MAPK. J Immunol 2009;182:1088-98.
5. Mok CK, Lee DC, Cheung CY, Peiris M, Lau AS. Differential onset of apoptosis in influenza A virus H5N1- and H1N1-infected human blood macrophages. J Gen Virol 2007;88:1275-80.

YK Cheung 張英傑
SCS Cheng 鄭澤森
Y Ke 柯　岩
Y Xie 謝　雍

Key Messages

1. Two novel HLA-A2.1 specific H5N1 nucleoprotein epitopes (NP373-381 AMDSNTLEL and NP458-466 FQGRGVFEL) capable of activating cytotoxic T-cells in vitro were identified.

2. When the H5N1 nucleoprotein epitopes (NP373-381 AMDSNTLEL and NP458-466 FQGRGVFEL) were used with the single chain trimer system, they elicited effective cytotoxic T-cell responses against the corresponding nucleoprotein peptide-loaded cells in an HHD transgenic mouse model.

Department of Biology, The Hong Kong University of Science and Technology
YK Cheung, SCS Cheng, Y Ke, Y Xie

RFCID project number: 05050162

Principal applicant and corresponding author:
Prof Yong Xie
Department of Biology, The Hong Kong University of Science and Technology, Clear Water Bay, Kowloon, Hong Kong SAR, China
Tel: (852) 2358 7340
Fax: (852) 2358 1559
Email: boyxie@ust.hk

Human immunogenic T cell epitopes in nucleoprotein of human influenza A (H5N1) virusz

Introduction

An outbreak of a highly pathogenic avian virus, H5N1, occurred in Hong Kong and other Asian countries in 1997, 2003, and 2004 and claimed more than 20 human lives and caused huge economic losses in the poultry industries worldwide.[1] Developing a strategy to combat the H5N1 virus is imperative. One possible solution is to develop vaccines for humans against this virus.

In the influenza A virus, the nucleoprotein (NP) is a comparatively conserved protein, and only a few amino acid differences have been observed from most bird virus strains over the past 90 years. Because of its high conservancy during its evolution, NP is a target for T-cell immunity.[2] One promising approach is to develop direct DNA vaccination to stimulate T-cell immunity against NP.

The single chain trimer (SCT) system has been used to construct DNA vaccines.[3] Two novel HLA-A2 restricted epitopes, H5N1 NP373-381 AMDSNTLEL and NP458-466 FQGRGVFEL, were identified through bioinformatics analysis. The NP peptides NP373 and NP458 showed a high binding affinity towards human MHC class-I in T2-cells, and were capable of activating cytotoxic T-cells in human peripheral blood mononuclear cells. The potential for using the NP373 and NP458 peptide sequences as major DNA vaccine components supplemented with a SCT was investigated in a HHD transgenic mouse model. Results from cytotoxicity and ELISPOT assays indicated that the T-cells obtained from the vaccinated mice secreted a significant amount of IFN-γ in response to NP373 and NP458 and were capable of eliminating the corresponding peptide-loaded T2 cells. The finding of the novel potential immunogenic NP peptides provides valuable information for avian flu vaccine design and construction.

Methods

This study was conducted from 1 August 2006 to 31 October 2008. H5N1 NP peptides from the strain *H5N1-Thailand-human-2004* were predicted by the HLA peptide binding prediction program (SYFPEITHI). Nine 9-mer potential peptides were synthesised by solid-phase strategies. They were NP48 KLSDYEGRL, NP55 RLIQNSITI, NP158 GMDPRMCSL, NP189 MVMELIRMI, NP256 LIFLARSAL, NP275 CLPACVYGL, NP357 QLSTRGVQI, NP373 AMDSNTLEL, and NP458 FQGRGVFEL. LALLLLDRL was used as a positive control.

The selected N-protein peptides were tested by in vitro stimulation of human CD8+ T-cells. Purified CD8+ T-cells were primed with autologous dendritic cells loaded with NP. Autologous dendritic cells were prepared from monocytes cultured in AIM-V medium (Gibco) supplemented with human AB serum and cytokines. Purified NP protein was added on day 5 and maturation of dendritic cells was facilitated by addition of maturation cytokines. NP-loaded mature dendritic cells were co-cultured with the CD8+ T-cells in the presence of cytokines for 7 days. CD8+ T-cells were stimulated three times with protein-loaded dendritic cells. Activation of T-cells was investigated by intracellular cytokine staining and

detected by flow cytometrical analysis.

Plasmids including NP158HHDpBudCE4.1, NP189HHDpBudCE4.1, NP373HHDpBudCE4.1, and NP458HHDpBudCE4.1 were generated by PCR. The SCT gene—HHD—was constructed by connecting the leader sequence, human β_2- microglobulin, human HLA-A2.1 α-1, α-2 domains and mouse H-2D^b α-3 domain and cloned into pBudCE4.1. Plasmids encoding different peptide sequences were constructed by adding the corresponding DNA fragments after the leader sequence of the HHD by PCR. The N220HHDpBudCE4.1 expressing LALLLLDRL peptide (N220) was used as a control plasmid.[3]

To investigate the cell-mediated immune response triggered by the SCT-DNA vaccine, mice were sacrificed one week after the last vaccination. Splenocytes were cultured with the addition of corresponding target peptides and cytokines for 5 days. Splenocytes were seeded with TDA-labelled, peptide-loaded T2 cells. After incubation for 1 hour at 37ºC, the culture medium was collected and the fluorescent signals from the target cells were detected by Delfia EuTDA cytotoxicity reagents (Perkin Elmer) according to the procedures stated by the manufacturer. An ELISPOT assay was performed by seeding splenocytes in the presence of corresponding target peptides on an anti-mouse IFN-γ antibody coated 96-well nitrocellulose plate that was incubated for 24 hours. Subsequently, the plate was washed and incubated with a biotinylated anti-mouse IFN-γ antibody followed by streptavidin-AP solution. Spots developed after adding BCIP/NBT solution and the visible spots were counted by an ELISPOT reader.

Results and discussion

To find an immunogenic NP peptide sequence, nine potential peptides were predicted using the SYFPEITHI program. The potential for stimulating human CD8+ T-cells was also determined (Fig 1). Results from intracellular cytokine staining showed that the T-cells stimulated with NP189 (MVMELIRMI), NP373 (AMDSNTLEL), and NP458 (FQGRGVFEL) produced the highest number of CD8+ IFN-γ secreting T-cells, whereas the NP158 (GMDPRMCSL) produced the lowest number of CD8+ IFN-γ secreting T-cells. The N160 (LQLPQGTTL) peptide-loaded T2 cells were used as a negative control and did not show any significant changes.[3] As the natural processing and display of peptides on the protein contribute significantly to the level of immune responses,[4] the number of IFN-γ-secreting cells that reacted during intracellular cytokine staining was not high, compared to the number of the whole pool of CD8+ T-cells. During natural processing, the dendritic cells loaded with the whole NP based on its cross-presentation characteristic and presented all epitopes on the protein to the CD8+ T-cells.[5] For this reason, all the activated CD8+ T-cells should be responsive to the immunogenic epitopes on the NP, and the number of CD8+ T-cells responding to a single type of peptide becomes

comparably low. In our experiment, our target cells were loaded with a single type of target peptide. This may explain the low percentage of the corresponding peptide-specific CD8+ T-cells.

An animal experiment was performed to test the immunogenicity of the target peptides in vivo after the selection of four target peptides, namely NP158 (GMDPRMCSL), NP189 (MVMELIRMI), NP373 (AMDSNTLEL), and NP458 (FQGRGVFEL) [Fig 2]. Results from the cytotoxicity assay showed that the mice immunised with plasmids encoding NP373 and NP458 produced the highest percentage of cytotoxic response, which was similar to the positive control, N220. During a 1-hour incubation period, NP373 had 14% and 10% killing effect with the effector cell-to-target cell ratios of 50:1 and 10:1, respectively, and the NP458 had 13% and 9% killing effect with the effector cell-to-target cell ratios of 50:1 and 10:1, respectively. However, the killing effect of NP189 was comparatively low (7%) with an effector cell-to-target cell ratio of 50:1, which contradicted the result from the T2 cell binding assay and intracellular cytokine staining of primed CD8+ T cells. The killing effect of NP158 was low as we expected, being 3.7% with a 50:1 ratio. An ELISPOT assay was used to determine the recognition of the splenocytes to their corresponding peptides by secreting IFN-γ after animal immunisation. The largest number of spots was obtained from NP373 and NP458, which were 317 and 286, respectively. In contrast, only 46 and 16 spots were observed with NP189 and NP158, respectively. The results were very close to the negative control (20 spots). The immunogenicity of NP189 in mice was significantly low, which was also not consistent with the results of the intracellular cytokine staining. Nonetheless, the results from NP373 and NP458 were more than 19 times higher than those from NP189 and NP158.

The cytotoxicity assay and ELISPOT assay showed that the NP373-381 AMDSNTLEL and NP458-466 FQGRGVFEL are the most immunogenic peptides (Fig 3). The reactivity of the two peptides was consistent with all the tests during the process of epitope identification. Although NP189 showed good responses after in vitro stimulation of human CD8+ T-cells, it induced weak animal immunisation responses. This indicates that the in vitro system may not truly reflect the situation in vivo. Nonetheless, in vitro experiments are essential for acquiring the basic information on newly found immunogenic peptides since the testing of the peptides generally cannot be performed in clinical trials without extensive investigation. Therefore, we should explore other possible approaches to verify the characteristics of potential peptides. The antigen processing, presentation and CD8+ T-cell responses in an artificial environment can be investigated via in vitro stimulation of human CD8+ T-cells. The HHD transgenic mouse model is an appropriate animal model for investigating the effects of the peptide-HLA complex and corresponding T cell responses in an in vivo system.
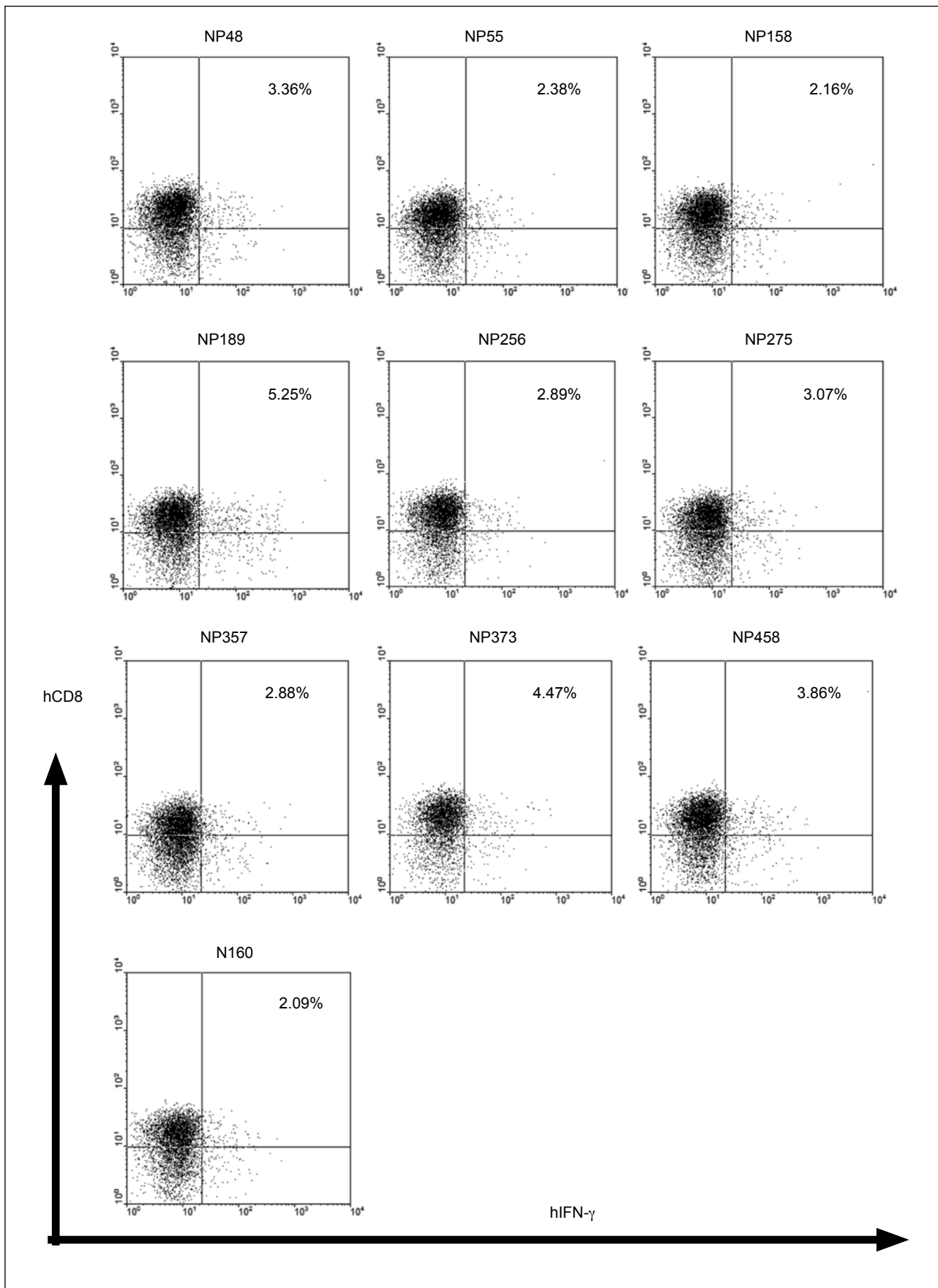
Fig 1. Intracellular cytokine staining owing to the secretion of IFN-γ from human CD8+ T-cells
Primed CD8+ T-cells are cultured with different target peptide-loaded T2 cells for 1 day and the number of IFN-γ secreting CE8+ T-cells is measured by PE-conjugated anti-CD8 and FITC-conjugated anti-IFN-γ antibodies. N160-loaded T2 cells serve as negative controls
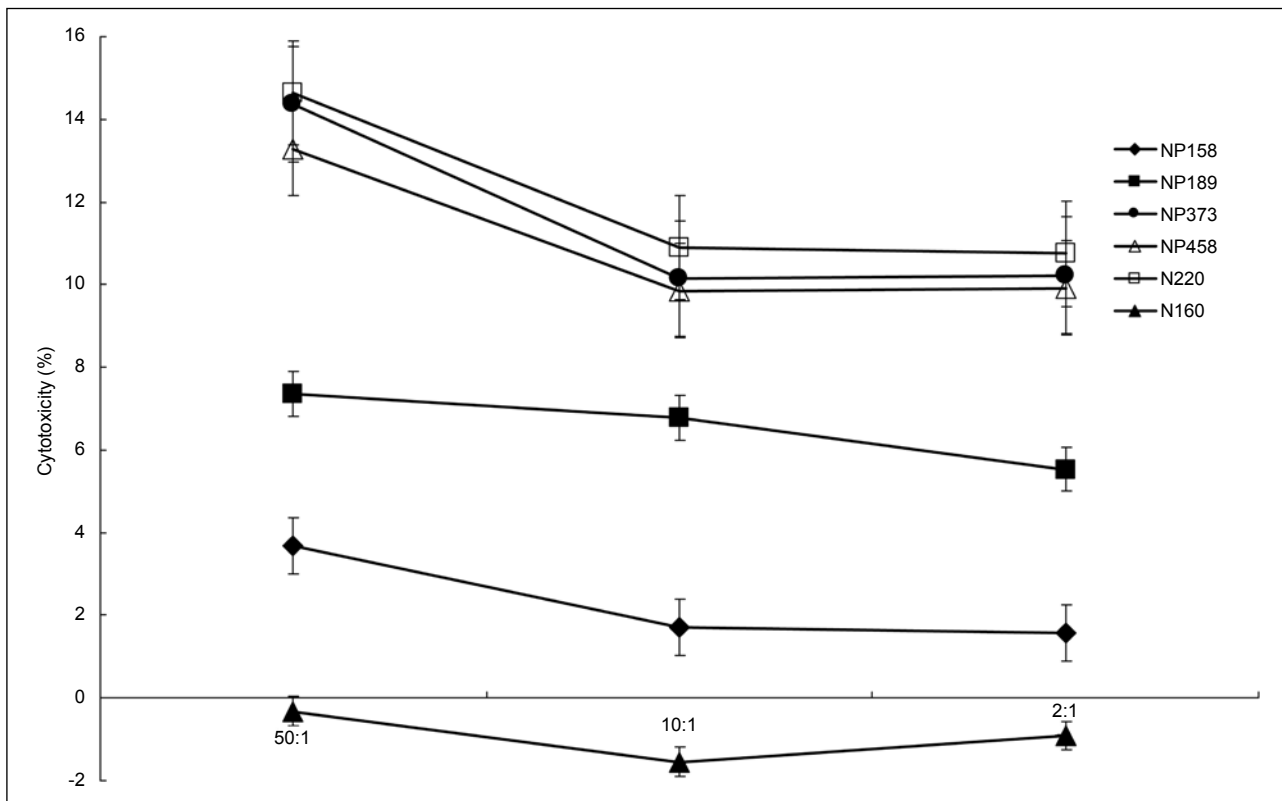
Fig 2. Percentage of specific killing of the target peptide-loaded T2 cells after immunisation
The X-axis indicates the ratios of the effector cells (splenocytes) to the target cells (peptide-loaded T2 cells). The Y-axis indicates the percentage of cytotoxicity. The cytotoxicity for the six groups of mice vaccinated with the various plasmids: NP158HHDpBudCE4.1, NP189 HHDpBudCE4.1, NP373HHDpBudCE4.1, and NP458HHDpBudCE4.1. N220HHDpBudCE4.1 is a positive control, whereas the mice vaccinated with the N220HHDpBud CE4.1 plasmid but tested with N160-loaded T2 cells are used as negative controls. Splenocytes from vaccinated animals are cultured with the corresponding peptides for 5 days. They are incubated with the corresponding peptide-loaded T2 cells for 1 hour. Means and SDs are shown (n=2, P<0.05)
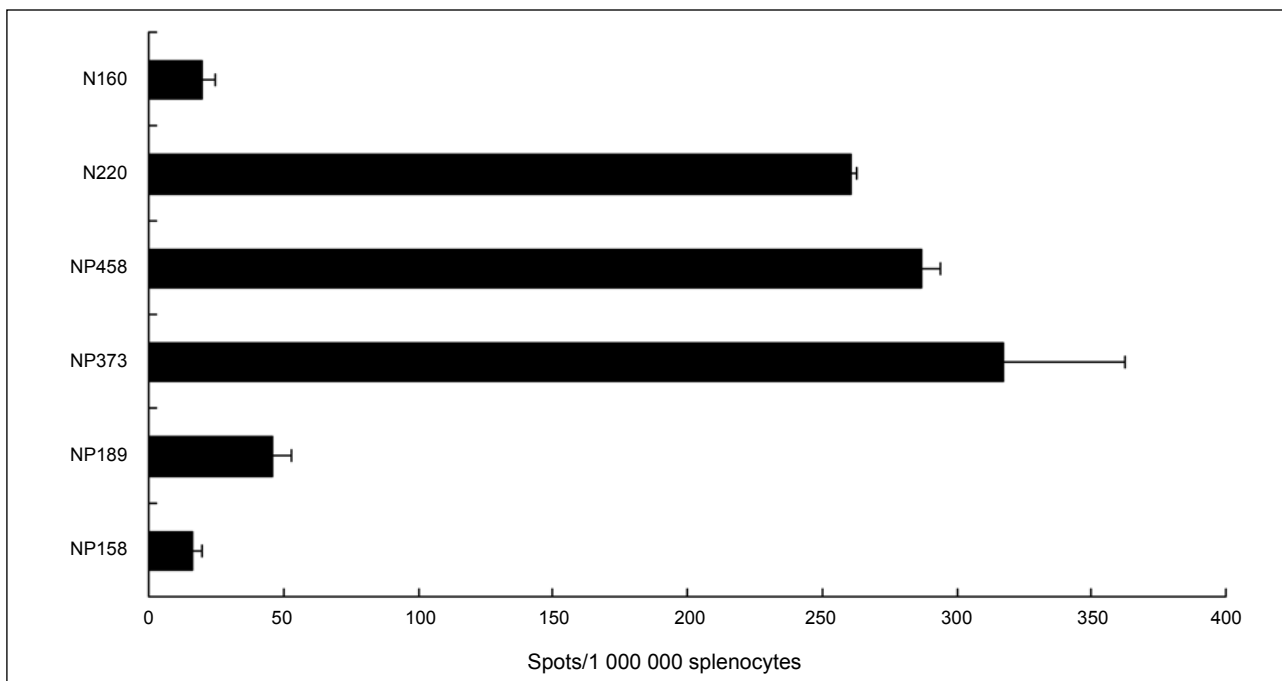
Fig 3. Results of the ELISPOT assay
Splenocytes obtained from mice vaccinated with the plasmids are cultured with corresponding peptides for 1 day and the secretion of IFN-γ is measured by the ELISPOT assay. The N160 peptide (LQLPQGTTL) is used as a negative control for the mice vaccinated with N220HHDpBudCE4.1. Means and SDs are shown (n=2) [three mice per group]

All our assays provided some information about the various peptide vaccine candidates and the results indicated that the NP373 and NP458 were capable of inducing strong immune responses both in vitro and in vivo. The NP373-381 AMDSNTLEL and NP458-466 FQGRGVFEL were two novel HLA-A2 T-cell epitopes found in (H5N1) viral NP.

Acknowledgement

References

1. Li KS, Guan Y, Wang J, et al. Genesis of a highly pathogenic and potentially pandemic H5N1 influenza virus in eastern Asia. Nature 2004;430:209-13.
2. Webster RG, Bean WJ, Gorman OT, Chambers TM, Kawaoka Y. Evolution and ecology of influenza A viruses. Microbiol Rev 1992;56:152-79.
3. Cheung YK, Cheng SC, Sin FW, Chan KT, Xie Y. Induction of T-cell response by a DNA vaccine encoding a novel HLA-A*0201 severe acute respiratory syndrome coronavirus epitope. Vaccine 2007;25:6070-7.
4. Dutoit V, Taub RN, Papadopoulos KP, et al. Multiepitope CD8(+) T cell response to a NY-ESO-1 peptide vaccine results in imprecise tumor targeting. J Clin Invest 2002;110:1813-22.
5. Cresswell P, Ackerman AL, Giodini A, Peaper DR, Wearsch PA. Mechanisms of MHC class I-restricted antigen processing and cross-presentation. Immunol Rev 2005;207:145-57.

PCY Woo 胡釗逸
KY Yuen 袁國勇
SKP Lau 劉嘉珮

Epidemiology of coronavirus-associated respiratory tract infections and the role of rapid diagnostic tests: a prospective studyz

Key Messages

1. Coronaviruses accounted for 1.6% (98/6272) of respiratory tract infections based on nasopharyngeal aspirate samples.
2. HCoV-OC43 was the most common coronavirus detected, followed by HCoV-NL63, CoV-HKU1, and HCoV-229E.
3. Although CoV-HKU1 infections were most often associated with the upper respiratory tract, more severe illness (pneumonia, acute bronchiolitis, and asthmatic exacerbation) may occur, especially in those with underlying disease. In young children, CoV-HKU1 infection is associated with a high rate of febrile seizures (50%).
4. CoV-HKU1 and HCoV-OC43 infections peaked in winter, in contrast to HCoV-NL63, which mainly occurred in early summer and autumn, but was absent in winter.
5. Reverse transcriptase polymerase chain reaction is useful for the rapid diagnosis of coronavirus infections.

Department of Microbiology, The University of Hong Kong
PCY Woo, KY Yuen, SKP Lau

RFCID project number: 04050222

Principal applicant:
Prof PCY Woo
Department of Microbiology, The University of Hong Kong, University Pathology Building, Queen Mary Hospital, Hong Kong SAR, China
Tel: (852) 2855 4892
Fax: (852) 2855 1241
Email: pcywoo@hkucc.hku.hk

Corresponding author:
Prof KY Yuen
Department of Microbiology, The University of Hong Kong, University Pathology Building, Queen Mary Hospital, Hong Kong SAR, China
Tel: (852) 2855 4892
Fax: (852) 2855 1241
Email: hkumicro@hkucc.hku.hk

Introduction

Four novel causative agents of respiratory tract infections have been identified: human metapneumovirus,[1] SARS coronavirus (SARS-CoV),[2] human coronavirus NL63 (HCoV-NL63),[3,4] and coronavirus HKU1 (CoV-HKU1).[5] Coronavirus HKU1 was first isolated in Hong Kong in January 2005 from a 71-year-old Chinese patient with pneumonia.[5] It has also been found in another patient with pneumonia,[5] suggesting that this virus is associated with respiratory tract infections. The clinical spectrum of CoV-HKU1 infection and its epidemiology in relation to other coronaviruses were unknown at that time. We examined the epidemiology and clinical spectrum of CoV-HKU1, HCoV-NL63, HCoV-OC43, and HCoV-229E infections in patients hospitalised for acute respiratory illness. Specific reverse transcriptase polymerase chain reaction (RT-PCR) assays were developed for the rapid diagnosis of coronavirus infections. The molecular epidemiology of CoV-HKU1 was analysed by sequencing of selected gene targets.

Methods

This study was conducted from 16 December 2005 to 15 December 2007. All prospectively collected nasopharyngeal aspirate (NPA) samples sent to the microbiology laboratory of Queen Mary Hospital during an 18-month period (April 2004 to September 2005) were included. All NPA samples were assessed for influenza A and B viruses, parainfluenza viruses types 1, 2 and 3, respiratory syncytial virus, adenovirus by direct immunofluorescence, and metapneumovirus by RT-PCR.[6,7] Those NPA samples negative for these respiratory viruses were subject to RT-PCR for coronaviruses. Once coronavirus was detected, corresponding patients were identified and their clinical features, laboratory results, and outcomes were analysed.

A total of 6272 NPA samples from patients with acute respiratory tract infections were identified. To evaluate the specificity of the RT-PCR assays, RNA of CoV-HKU1, HCoV-OC43, HCoV-229E, HCoV-NL63, and SARS-CoV, as well as RNA extracted from 200 NPA sample positive for influenza A and B viruses, parainfluenza viruses 1-3, respiratory syncytial virus (RSV), or adenovirus antigens were also subject to RT-PCR.

Upon receipt of samples, viral RNA was extracted using QIAamp Viral RNA Mini Kit (QIAgen, Hilden, Germany) within 10 hours. Reverse transcription was performed using random hexamers and the SuperScript II kit (Invitrogen, San Diego [CA], USA).[5,8] For coronaviruses, PCR was performed using four sets of primers specifically designed to amplify CoV-HKU1, HCoV-OC43, HCoV-229E, and HCoV-NL63, targeted to the same region of the RNA-dependent RNA polymerase (*pol*) gene. The sequences of the PCR products were compared with the sequences of the *pol* genes of coronaviruses in the GenBank database. To determine the molecular epidemiology of CoV-HKU1, the complete *pol*, spike (S) and N genes of CoV-HKU1 from 13 patients were amplified and sequenced. Phylogenetic tree construction was performed using the neighbour-joining

method with GrowTree using the Jukes-Cantor correction (Genetics Computer Group).

Since a high rate of febrile seizures was noted in patients with CoV-HKU1 infection, the relative frequency of febrile convulsion, maximum temperature, duration of fever, and duration of hospitalisation in children at risk of febrile seizures (aged 6 months to 5 years) with different respiratory virus infections were analysed by review of clinical records. Comparisons were made among the various groups of patients with respiratory virus infections.

Results

Coronaviruses were detected in 98 (1.61%) of the 6272 NPA samples. Using RT-PCR, 13 were positive for CoV-HKU1, 61 for HCoV-OC43, five for HCoV-229E, and 19 for HCoV-NL63. None of the 200 NPAs positive for influenza A and B viruses, parainfluenza viruses 1-3, RSV, or adenovirus antigens was RT-PCR positive for coronaviruses. The PCR reactions were specific for the corresponding coronavirus.

No epidemiological linkage was identified in 13 cases: 10 occurred in autumn or winter (November to February) and three in spring or summer (April to July). The median patient age was 3 (range, 1.6-87) years; most patients were children. Common presenting symptoms were fever, running nose, and cough with or without sputum. All had upper respiratory infections, except for two who had lower respiratory tract infections and abnormalities on chest radiographs (one had bilateral lower zone haziness, and another had perihilar haziness). Eight patients had underlying diseases. Two patients had recent travel histories. Two patients were smokers. Five children had febrile seizures and two others with underlying epilepsy had breakthrough seizures. Febrile seizures occurred in 38% of patients with CoV-HKU1 infections, 18% of those with HCoV-NL63 infections, and 6% of those with HCoV-OC43 infections. In patients with pre-existing epilepsy, breakthrough seizures occurred in those with CoV-HKU1 and HCoV-NL63 infections. Both febrile and breakthrough seizures were more common in patients with CoV-HKU1 infections than in those with HCoV-OC43 infections (P<0.05).

The seasonality of CoV-HKU1 was compared to that of other coronaviruses. CoV-HKU1 and HCoV-OC43 mainly occurred in the autumn and winter months, whereas HCoV-NL63 mainly occurred in the summer and autumn.

A total of 629 children aged 6 months to 5 years were hospitalised for acute respiratory virus infections during the study period. The rate of febrile seizures was significantly higher in children with CoV-HKU1 infections than in those with HCoV-OC43, adenovirus, human parainfluenza virus 1, or respiratory syncytial virus infections (P<0.05). There was no significant difference in the maximum temperature

and duration of hospitalisation between CoV-HKU1 infections and other virus infections. Children with other respiratory virus infections, except HCoV-OC43, had longer duration of fever than those infected with CoV-HKU1 did (P<0.05).

Sequencing and phylogenetic analysis showed the presence of at least two genotypes which are better distinguished based on S and N genes than the *pol* gene. Seven of the 13 strains belonged to genotype A and the other six to genotype B.

Discussion

Coronavirus infections were present in 1.6% of NPA samples, with HCoV-OC43 being the most prevalent, followed by HCoV-NL63 and CoV-HKU1 and then HCoV-229E. CoV-HKU1 was responsible for 0.2% of patients with acute respiratory illness. In old people with major underlying diseases, CoV-HKU1 mostly caused pneumonia.[8] In young children with or without underlying diseases, upper respiratory tract infection was the most common presentation. CoV-HKU1 infections occasionally resulted in more severe illness (acute bronchiolitis and asthmatic exacerbation). There may be selection bias especially for adults, as only hospitalised patients were included. Young children are often admitted to hospital even for mild illness, whereas adults with mild disease are usually treated in the primary care sector. This may have over-estimated the severity of such infections in adults.

HCoV-NL63 infections appeared in early summer and peaked in autumn, but were absent in winter. Similarly, CoV-HKU1 infections increased in autumn and peaked in winter, and a few cases occurred in spring to early summer, unlike HCoV-OC43 infections that no cases were observed in the other seasons. The seasonal pattern of HCoV-229E could not be determined because of the small number of cases. Continuous studies carried out over a number of years are required to ascertain the seasonal and any possible inter-year variation in the relative incidence of the different coronaviruses.

Specific RT-PCR was useful for the rapid diagnosis of coronavirus infections. Especially for CoV-HKU1, it may provide a clue to anticipating febrile seizures in children with acute respiratory tract infections. In fact, half of the affected children had febrile seizures, which was the highest rate among other studied respiratory virus infections. Although there was no significant difference in the maximum temperature caused by CoV-HKU1 and other respiratory viruses, there was a trend for lower temperatures with the coronaviruses compared to influenza A and adenovirus. Therefore, it is unlikely that the high rate of febrile seizures associated with CoV-HKU1 and HCoV-NL63 infections can be explained by differences in the extent of fever. A novel amino acid substitution in the haemagglutinin gene of influenza A correlates with acute

encephalopathy.[9] Nonetheless, further studies with a much larger sample size are needed to evaluate the significance of the present findings. If such association between febrile seizures and CoV-HKU1 can be confirmed, investigation for specific neurotropic or epileptogenic factors in CoV-HKU1 and those respiratory viruses with a propensity to cause febrile seizures can be carried out.

At least two distinct genotypes of CoV-HKU1 were revealed by sequencing the S and N genes, whereas the *pol* gene is less discriminative for such classification. The two genotypes co-circulated during the winter, a phenomenon similar to HCoV-NL63 demonstrated in different geographical areas.[4,10,11] The S and N genes may be more useful for genotyping of CoV-HKU1.

Acknowledgements

References

1. van den Hoogen BG, de Jong JC, Groen J, et al. A newly discovered human pneumovirus isolated from young children with respiratory tract disease. Nat Med 2001;7:719-24.
2. Peiris JS, Lai ST, Poon LL, et al. Coronavirus as a possible cause of severe acute respiratory syndrome. Lancet 2003;361:1319-25.
3. Fouchier RA, Hartwig NG, Bestebroer TM, et al. A previously undescribed coronavirus associated with respiratory disease in humans. Proc Natl Acad Sci U S A 2004;101:6212-6.
4. van der Hoek L, Pyrc K, Jebbink MF, et al. Identification of a new human coronavirus. Nat Med 2004;10:368-73.
5. Woo PC, Lau SK, Chu CM, et al. Characterization and complete genome sequence of a novel coronavirus, coronavirus HKU1, from patients with pneumonia. J Virol 2005;79:884-95.
6. Peiris JS, Tang WH, Chan KH, et al. Children with respiratory disease associated with metapneumovirus in Hong Kong. Emerg Infect Dis 2003;9:628-33.
7. Woo PC, Chiu SS, Seto WH, Peiris M. Cost-effectiveness of rapid diagnosis of viral respiratory tract infections in pediatric patients. J Clin Microbiol 1997;35:1579-81.
8. Woo PC, Lau SK, Tsoi HW, et al. Clinical and molecular epidemiological features of coronavirus HKU1-associated community-acquired pneumonia. J Infect Dis 2005;192:1898-907.
9. Mori SI, Nagashima M, Sasaki Y, et al. A novel amino acid substitution at the receptor-binding site on the hemagglutinin of H3N2 influenza A viruses isolated from 6 cases with acute encephalopathy during the 1997-1998 season in Tokyo. Arch Virol 1999;144:147-55.
10. Bastien N, Anderson K, Hart L, et al. Human coronavirus NL63 infection in Canada. J Infect Dis 2005;191:503-6.
11. Chiu SS, Chan KH, Chu KW, et al. Human coronavirus NL63 infection and other coronavirus infections in children hospitalized with acute respiratory disease in Hong Kong, China. Clin Infect Dis 2005;40:1721-9.

KY Yuen 袁國勇
SKP Lau 劉嘉珮
PCY Woo 胡釗逸

Wild animal surveillance for coronavirus HKU1 and potential variants of other coronavirusesz

Key Messages

1. Although CoV-HKU1 was not identified in any of the studied animals, a coronavirus closely related to SARS-CoV (bat-SARS-CoV) was identified in 23 (19%) of 118 wild Chinese horseshoe bats by reverse transcriptase polymerase chain reaction (RT-PCR).
2. Complete genome sequencing and phylogenetic analysis showed that bat-SARS-CoV formed a distinct cluster with SARS-CoV as group 2b coronaviruses, distantly related to known group 2 coronaviruses.
3. Most differences between the bat-SARS-CoV and SARS-CoV genomes were observed in the spike gene. The presence of a 29-bp insertion in ORF 8 of bat-SARS-CoV genome, not in most human SARS-CoV genomes, suggests that it has a common ancestor with civet SARS-CoV.
4. Antibody against recombinant bat-SARS-CoV nucleocapsid protein was detected in 84% of Chinese horseshoe bats using an enzyme immunoassay. Neutralising antibody to human SARS-CoV was also detected in those with lower viral loads.
5. This study also revealed a previously unknown diversity of coronaviruses in bats, which are important natural reservoir for coronaviruses including SARS-CoV-like viruses.

Department of Microbiology, The University of Hong Kong
KY Yuen, SKP Lau, PCY Woo

RFCID project number: 04050232

Principal applicant and corresponding author:
Prof Kwok-yung Yuen
Department of Microbiology, The University of Hong Kong, University Pathology Building, Queen Mary Hospital, Hong Kong SAR, China
Tel: (852) 2855 4892
Fax: (852) 2855 1241
Email: hkumicro@hkucc.hku.hk

Introduction

Coronaviruses are found in a wide variety of animals in which they cause respiratory, enteric, hepatic, and neurological diseases of varying severity. Owing to their unique mechanism of viral replication, coronaviruses have a high frequency of recombination. This tendency for frequent recombination and high mutation rates enable them to adapt to new hosts and ecological niches. Although the isolation of SARS-CoV from caged animals (Himalayan palm civets and a raccoon dog) from wild animal live markets in mainland China suggests that they are the reservoir from which the SARS epidemic originated,[1] several lines of evidence suggest that the civet may have served as an amplification host only for SARS-CoV.[2-5] In January 2005, we reported the discovery of a novel coronavirus, coronavirus HKU1 (CoV-HKU1), from a patient with pneumonia in Hong Kong.[6] The patient was a 71-year-old Chinese man who had just returned from Shenzhen, China three days before admission. The patient's recent travel history raised a suspicion that he had acquired the virus directly or indirectly through contact with wild animals. We therefore conducted a one-year wild animal surveillance study in Hong Kong to find possible animal reservoirs for CoV-HKU1 or other coronaviruses. Upon identification of coronaviruses, complete genome sequencing and serological studies were performed.

Methods

This study was conducted from 16 December 2005 to 15 December 2007 and entailed a one-year surveillance of non-caged mammals in the wilds of Hong Kong. The study was performed in collaboration with the Agriculture, Fisheries and Conservation Department, and the Food and Environmental Hygiene Department. It was approved by the Committee on the Use of Live Animals in Teaching and Research, The University of Hong Kong.

A total of 489 wild animals, including 309 bats, 160 rodents and 20 monkeys were captured from various locations in Hong Kong. As initial surveillance results in bats were more promising, more bats were captured than originally planned to replace the reduced number of captured monkeys. All animals were released back to the wild after sample collection.

Swabs were taken and kept in viral transport medium at 4°C before processing.[7] Where possible, blood was collected from the bats for serological studies by a veterinary surgeon. All nasopharyngeal and anal swabs were tested for coronavirus RNA by RT-PCR, using conserved primers targeted to a 440-bp fragment of the *pol* gene.[8] The sequences of the PCR products were compared with known sequences of the *pol* genes of coronaviruses in the GenBank. Based on the initial results, attempts to isolate bat-SARS-CoV were made by inoculating RT-PCR positive specimens to FRhK-4, HRT-18G, Huh-7, Vero E6, C6/36, and Caco-2 cells, as well as chicken embryonated eggs.

The complete genome of bat-SARS-CoV was sequenced using RNA extracted from anal swabs of three bats as a template. The complete S genes of bat-SARS-CoV from 14 positive samples, with adequate amounts of RNA available, were sequenced using primers targeted to S. Quantitative RT-PCR

was used to determine the viral loads in positive samples. Serological studies were performed using western blot and enzyme immunoassay (EIA) based on $(His)_6$-tagged recombinant N protein of bat-SARS-CoV. Neutralisation assays to SARS-CoV were also performed.

Results

A total of 309 bats of 13 species, 160 rodents of 5 species, and 20 monkeys (*Macaca mulatta*) were sampled. RT-PCR for a 440-fragment of *pol* gene of coronaviruses was positive in anal swabs from 39 bats. None of the specimens from rodents and monkeys was positive. Sequencing results suggested the presence of at least three different coronaviruses, including one closely related to SARS-CoV. This virus possessed 88% nucleotide identities to SARS-CoV and was found in 23 Chinese horseshoe bats.[9] Attempts to stably passage these viruses in cell lines were unsuccessful.

Phylogenetic analysis showed that the bat-SARS-CoV, together with SARS-CoV from humans and civets, belongs to a group distantly related to known group 2 coronaviruses. The three genomes possessed 88% nucleotide and 93% amino acid identities to 10 human and civet SARS-CoV with genome sequences available. Most differences between the bat-SARS-CoV genomes and human and civet SARS-CoV genomes were observed in the S gene, ORF 3, and ORF 8. Compared to SARS-CoV from humans and civets, there were 11 insertions and 15 deletions in the bat-SARS-CoV genome. The 29-bp region, deleted in most human SARS-CoV, is present, as in civet SARS-CoV.

Among tested sera from Chinese horseshoe bats, 12 (67%) of 18 were positive for bat-SARS-CoV antibody by western blot and 31 (84%) of 37 by EIA with titre ≥1:400; but only 8 (42%) of 19 for human SARS-CoV neutralising antibody with titre ≥1:20. Interestingly, those with neutralising antibody had lower viral loads in their anal swabs (P=0.016, Student's *t* test).

Discussion

Although none of the animal samples possessed coronavirus closely related to CoV-HKU1, the bat-SARS-CoV was identified, which is closely related to SARS-CoV from humans and civets, suggesting that bats are likely the animal reservoir of SARS-CoV-like viruses. Moreover, a diversity of coronaviruses in bats was also discovered and warrants further investigations. Bat-SARS-CoV was identified from 23 anal swabs from the species *R sinicus*; 67% and 84% of tested sera from Chinese horseshoe bats were positive for antibodies against recombinant bat-SARS-CoV N protein by western blot and EIA, respectively. Further studies are required to find out if there are yet unidentified intermediate hosts between bats and civets.

Hong Kong has extensive natural areas with 52 terrestrial

mammals, including 22 bat species. The Chinese horseshoe bat (*R sinicus*), belonging to the family *Rhinolophidae* of the order *Chiroptera* under *Microphiroptera* (microbat), is an insectivorous species widely distributed in forested areas throughout Hong Kong and China (http://www. hkbiodiversity.net). The species *R sinicus* was previously called the *R rouxii* subspecies *sinicus* but recent karyotyping study has elevated its status to a separate species. Although no data on its migration patterns are available, members of *Rhinolophus* may migrate up to 30 km for hibernation in winter. Interestingly, the nearest wild life market in Shenzhen found to have animals with SARS-CoV is only 17 km away from the locations with bats harbouring bat-SARS-CoV in Hong Kong. The phylogenetic distance from SARS-CoV and the presence of the 29-bp insertion in ORF 8 of bat-SARS-CoV genomes suggest that bat-SARS-CoV is unlikely to result from transmission of SARS-CoV from humans to bats. Instead, bat-SARS-CoV and civet SARS-CoV are likely to have a common ancestor. Nevertheless, the direction of inter-species transmission of SARS-CoV-like viruses or their ancestral relationships cannot be directly inferred. Continuous surveillance for coronaviruses in these flying mammals with roosting behaviour is necessary to assess their potential threats to human health.

Acknowledgements

References

1. Guan Y, Zheng BJ, He YQ, et al. Isolation and characterization of viruses related to the SARS coronavirus from animals in southern China. Science 2003;302:276-8.
2. Song HD, Tu CC, Zhang GW, et al. Cross-host evolution of severe acute respiratory syndrome coronavirus in palm civet and human. Proc Natl Acad Sci U S A 2005;102:2430-5.
3. Li W, Zhang C, Sui J, et al. Receptor and viral determinants of SARS-coronavirus adaptation to human ACE2. EMBO J 2005;24:1634-43.
4. Yang ZY, Werner HC, Kong WP, et al. Evasion of antibody neutralization in emerging severe acute respiratory syndrome coronaviruses. Proc Natl Acad Sci U S A 2005;102:797-801.
5. Tu C, Crameri G, Kong X, et al. Antibodies to SARS coronavirus in civets. Emerg Infect Dis 2004;10:2244-8.
6. Woo PC, Lau SK, Wong BH, et al. False-positive results in a recombinant severe acute respiratory syndrome-associated coronavirus (SARS-CoV) nucleocapsid enzyme-linked immunosorbent assay due to HCoV-OC43 and HCoV-229E rectified by Western blotting with recombinant SARS-CoV spike polypeptide. J Clin Microbiol 2004;42:5885-8.
7. Poon LL, Chu DK, Chan KH, et al. Identification of a novel coronavirus in bats. J Virol 2005;79:2001-9.
8. Woo PC, Lau SK, Chu CM, et al. Characterization and complete genome sequence of a novel coronavirus, coronavirus HKU1, from patients with pneumonia. J Virol 2005;79:884-95.
9. Lau SK, Woo PC, Li KS, et al. Severe acute respiratory syndrome coronavirus-like virus in Chinese horseshoe bats. Proc Natl Acad Sci U S A 2005;102:14040-5.

TF Leung 梁廷勳
PKS Chan 陳基湘
WKG Wong 黃永堅
M Ip 葉碧瑤
WTF Cheng 鄭偉才
PC Ng 伍百祥

Human coronavirus NL63 in children: epidemiology, disease spectrum, and genetic diversityz

Key Messages

1. Human coronaviruses (HCoVs) were detected in 2.5% of 2982 local children hospitalised for acute respiratory infections in 2005 to 2007.
2. Using the 'pancoronavirus' reverse transcription-polymerase chain reaction assay, detection rates were 0.6% for HCoV-NL63, 1.2% for HCoV-OC43, 0.5% for HCoV-HKU1, and 0.2% for HCoV-229E. Notably, HCoV-NL63 infections were significantly more common among children hospitalised in 2006/2007 (1.2%) than in 2005/2006 (0.3%).
3. The peak season for HCoV-NL63 infection was autumn (September to October).
4. HCoV-NL63 infection was associated with younger age, croup, febrile convulsion, and acute gastroenteritis. Such disease associations were not found with the other three HCoVs.
5. Most local HCoV-NL63 isolates were closely related to the prototype strain in Netherlands (NL496), but a few were phylogenetically distinct from the major cluster.

The Chinese University of Hong Kong, Prince of Wales Hospital:
Department of Paediatrics
TF Leung, WKG Wong, WTF Cheng, PC Ng
Department of Microbiology
PKS Chan, M Ip

RFCID project number: 04050372

Principal applicant and corresponding author:
Dr Ting Fan Leung
Department of Paediatrics, 6/F, Clinical Sciences Building, Prince of Wales Hospital, 30-32 Ngan Shing Street, Shatin, NT, Hong Kong SAR, China
Tel: (852) 2632 2981
Fax: 2636 0020
Email: tfleung@cuhk.edu.hk

Introduction

Acute respiratory tract infections (RTIs) account for considerable morbidity and mortality in humans. Even in the most comprehensive studies, a causative agent (either viral or non-viral) can be identified in only 85% of the patients. This may be due to the limitations of diagnostic assays, but a proportion of RTIs may be caused by unknown pathogens. Coronaviruses, a genus of the *Coronaviridae* family, are enveloped viruses with a large plus-strand RNA genome. Up to the year 2003, three serologically distinct groups of human coronaviruses (HCoVs) had been described: HCoV-229E, HCoV-OC43, and SARS-CoV. Two independent groups identified HCoV-NL63 in the following year.[1,2] Among Caucasians, this virus could be detected in 2 to 8.8% of patients with acute RTIs of 'unknown aetiology'. Most positive isolates were found in winter, and this virus might be associated with a wide range of acute RTIs (from common cold to pneumonia). Nonetheless, the epidemiology, seasonality, and clinical features of HCoV-NL63 infection remain unclear.

We aimed to (1) understand the seasonality and epidemiology of HCoV-NL63 in local children, (2) characterise the genetic diversity of HCoV-NL63 circulating in Hong Kong, and (3) delineate demographic, clinical, and laboratory parameters of such infections in our population.

Methods

This two-phased study was conducted from 1 February 2006 to 1 July 2008. In the first phase, about 2000 systematically selected nasopharyngeal aspirate (NPA) samples from hospitalised children (<18 years old) with acute RTIs during a 12-month period in 2005/2006 were retrospectively screened for all types of HCoVs. In the second phase, NPA samples from the first 20 hospitalised children in every week with un-identified common respiratory viruses were prospectively collected between December 2006 and November 2007. Clinical and demographic data of 1001 subjects with virus-negative NPA samples were obtained. Laboratory tests were requested when clinically indicated. No therapeutic intervention was carried out. Patients' parents gave informed written consent, and the Joint CUHK-NTEC Clinical Research Ethics Committee approved this study.

Identification of HCoVs in nasopharyngeal aspirate samples

The NPA samples were stored at -80°C or analysed fresh. Extracted RNA was transcribed into cDNA using random hexamers with Superscript III RNase H-reverse transcriptase (Invitrogen, Carlsbad [CA], USA). For the detection of HCoVs, a low-stringency 'pancoronavirus' RT-PCR assay targeted against the polymerase gene was developed.[3] A mixture of 12 pairs of forward and reverse primers were designed from the sequence alignment of 15 closely related CoVs. PCR reactions were carried out in a total volume of 25 μL containing 2 μL cDNA, 0.25 μL HotStart Taq, 10 μM of each deoxynucleotide triphosphate and 0.6 μL of each primer mix. Samples were denatured at 94°C for 10 minutes followed by 35 cycles of 94°C for 40 seconds, 55°C for 40 seconds and 72°C for 60 seconds, and a final extension at 72°C for 10 minutes. The 228-bp PCR products were electrophoresed in 2% agarose gels. Following this, amplification products

positive for HCoVs were purified using MicroSpin S400 HR column (Pharmacia, Biotech, Sweden) and subjected to gene sequencing using the forward primer mix and BigDye Terminator Cycle sequencing kit v.3 on an ABI-3130 Sequencer (Applied Biosystems, Foster City [CA], USA). The gene sequence thus obtained from each subject was compared with publicly accessible sequences, using nucleotide blast software of Blastn Program (http://www. ncbi.nlm.nih.gov/BLAST) to identify the HCoV with the highest percentage of sequence homology.

Genetic diversity of HCoV-NL63 isolates

HCoV-NL63-positive samples were re-amplified for the partial 1a and partial spike genes using nested-PCR.[3] The same PCR reaction mixes as above were used. Samples were denatured at 94ºC for 5 minutes followed by 35 cycles

of 94ºC for 40 seconds, 50ºC for 40 seconds, and 72ºC for 60 seconds, and a final extension at 72ºC for 10 minutes. The expected PCR products were 525 bp (1a gene) and 663 bp (spike gene), respectively. The PCR products obtained were purified using a MicroSpin S400 HR column, and then subjected to direct sequencing on an ABI-3130 Sequencer.

Phylogenetic analysis

Sequence alignments of partial 1a and spike gene sequences of HCoV-NL63[1] were generated by CLUSTALW (version 1.8). Phylogenetic trees were constructed by the neighbour-joining method, rooted phylogenetic trees were generated using PAUP* (version 4.0; beta). The robustness of phylogenetic trees was assessed by bootstrap analysis. Bootstrap values were determined with 1000 resamplings of the data sets. Bootstrap values greater than 70% provide

Table 1. Identification of HCoVs among nasopharyngeal aspirate–negative subjects in 2005/2006 and 2006/2007

HCoV serotype	No. (%) of positive subjects		P value*
	2005/2006 (n=1802)	2006/2007 (n=1001)	
HCoV-NL63	5 (0.3)	12 (1.2)	0.006
HCoV-OC43	25 (1.4)	12 (1.2)	0.805
HCoV-229E	6 (0.3)	0	0.095
HCoV-HKU1	10 (0.6)	4 (0.4)	0.781
Total	46 (2.6)	28 (2.8)	0.792

* Chi squared test for all except for HCoV-229E, which used the Fisher exact test
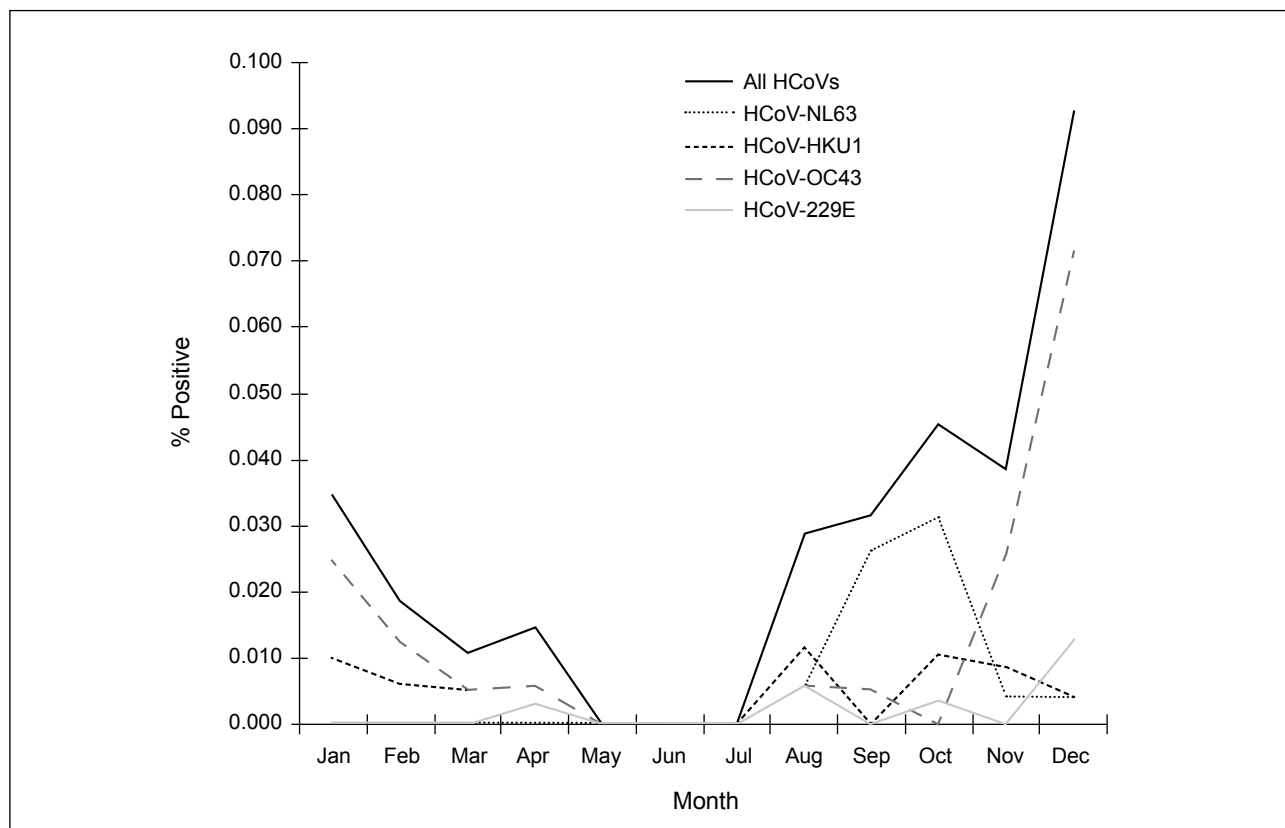
Fig. Seasonality pattern for all HCoVs and individual serologic types in nasopharyngeal aspirate samples collected during the 24-month period in 2005 to 2007

Table 2. HCoV-NL63-infected and nasopharyngeal aspirate (NPA)–negative cases recruited during the 12- onth period in 2006/2007

Feature	HCoV-NL63-infected*	NPA-negative*	P value[†]
Patient age (years)	0.9 (0.6-1.0)	2.0 (0.9-5.0)	0.007
Male	41.7	46.3	0.751
Duration of hospitalisation (days)	2.0 (1.0-2.8)	2.0 (1.0-4.0)	0.320
Duration of fever (days)	2.0 (1.0-3.0)	2.0 (1.0-4.0)	0.258
Fever on admission	100	90.0	0.317
Abnormal chest radiograph	25.0	38.3	0.441
Discharge diagnoses			
Upper respiratory tract infection	33.3	34.0	0.960
Acute tonsillitis	0	2.1	0.614
Croup	8.3	0.3	<0.001
Acute bronchiolitis	8.3	5.8	0.711
Acute bronchitis	0	0.6	0.784
Asthma exacerbations	8.3	6.5	0.803
Pneumonia	0	14.3	0.157
Acute otitis media	0	0.8	0.751
Febrile convulsion	16.7	3.9	0.027
Acute gastroenteritis	33.3	12.2	0.028
Roseola infantum	0	2.8	0.557
Viral illness	8.3	4.7	0.552
Laboratory results			
Haemoglobin (g/dL)	12.3 (11.3-13.6)	12.3 (11.4-13.0)	0.726
Platelet count (x10^9/L)	347.0 (285.0-431.8)	293.0 (231.0-374.3)	0.110
Total white cell count (x10^9/L)	9.5 (8.4-11.4)	9.5 (6.6-13.4)	0.864
Absolute neutrophil count (x10^9/L)	4.49 (2.55-6.77)	5.39 (3.10-8.93)	0.300
Absolute lymphocyte count (x10^9/L)	2.82 (2.21-4.55)	2.53 (1.58-4.10)	0.234
Highest C-reactive protein (mg/L)	7.7 (1.4-82.9)	23.2 (7.3-66.1)	0.137

* Data are presented as median (interquartile range) or %
[†] Analysed by Mann-Whitney *U* test for numerical variables, and Chi squared or Fisher exact test for categorical data

significant evidence for phylogenetic grouping. The final tree was obtained with the FigTree program (version 1.2.2) (http://tree.bio.ed.ac.uk/software/figtree/).

Virus isolation for HCoV-NL63

Although there is currently no established method for isolating HCoV-NL63, we attempted to propagate five HCoV-NL63 in a few commonly used cell lines including Vero, MDCK, LLC-MK2, HeLa, Hep2, RD, and MRC-5 cells. Briefly, 0.3 mL of NPA was inoculated onto each cell monolayer and incubated at 37ºC with maintenance medium containing 1 µg/mL of trypsin. Cell monolayers were examined daily for 14 days for cytopathic effect. The medium changed on days 5 to 7. All specimens were blind passaged once.

Results

Of 1981 NPA samples, 1802 were NPA negative and 179 were patients with acute bronchiolitis, bronchitis or asthma exacerbations whose NPA had ≥1 respiratory virus by direct immunofluorescence. The mean±standard deviation age of NPA-positive and NPA-negative subjects were 2.6±2.8 and 3.5±3.6 years, respectively (P=0.001). NPA-negative patients were more likely to have fever (P=0.002), low SaO$_2$ (P=0.010), abnormal chest radiograph (P<0.001), and oxygen supplementation (P<0.001). The two groups were comparable for their vital signs, but NPA-negative cases had higher total white cell counts (P<0.001), absolute neutrophil counts (P<0.001), and peak serum C-reactive protein levels (P=0.019).

Detection of HCoV-NL63

Our 'pancoronavirus' RT-PCR identified 74 (2.5%) cases as having HCoVs among all 2982 NPA samples. Of these HCoV-infected patients, 46 and 28 came from the retrospective and prospective cohorts, respectively (P=0.792). A total of 17 (0.6%) patients with HCoV-NL63 were identified in 2005 to 2007, being significantly more common among children hospitalised in 2006/2007 than in 2005/2006 (1.2% vs 0.3%, P=0.006, Table 1). The detection rates for the other three types of HCoVs were comparable in these 2 years. In our retrospective cohort, none of the 179 NPA-positive patients with acute bronchiolitis, bronchitis or asthma exacerbations had co-infection with HCoV-NL63.

Seasonality and clinical features of HCoV-NL63 infection

A total of 74 HCoVs were identified in the combined 24-month study period from 2005 to 2007. The incidence of HCoV infections among our hospitalised children peaked in winter (November to January), which was mainly associated with HCoV-OC43 infection (Fig). In contrast, the peak season for HCoV-NL63 infection in local children occurred earlier in autumn (September to October) during the same period.

In view of any possible recall bias, five patients with HCoV-NL63 infection in our retrospective cohort were not counted. Patients with HCoV-NL63 infection were younger (P=0.007), and more likely to have had croup (P<0.001), febrile convulsion (P=0.027) and acute gastroenteritis (P=0.028) [Table 2]. Such disease associations were not

detected with the other three HCoVs (P>0.1). Nonetheless, HCoV-NL63 was not associated with any significant laboratory abnormality.

Phylogenetics of HCoV-NL63 isolates

The majority of HCoV-NL63 isolates circulating in Hong Kong in 2005 to 2007 were closely related phylogenetically to strains that have been reported in Belgium (BE-03-1153, BE-03-64880) and the Netherlands (NL72). A small group of HCoV-NL63 strains (CU U0348, CU X091, CU P208, CU U0355) that circulated in Hong Kong were distinct from the major cluster.

Virus isolation for HCoV-NL63

Despite blind passage, none of the cell lines used showed evidence of virus growth either by cytopathic effect or RT-PCR determination at the end of incubation.

Discussion

Two groups of researchers independently identified HCoV-NL63 in 2004.[1,2] This virus was present in 2 to 8.8% of respiratory specimens from patients with acute RTIs. Another study suggested that this virus was less common (0.4%).[4] There are four major serologically distinct groups of HCoVs: HcoV-OC43, HCoV-NL63, HCoV-229E, and HCoV-HKU1. In this study, we developed a low-stringency RT-PCR assay for the simultaneous detection of these HCoVs. This 'pancoronavirus' system may also be able to identify previously unknown CoVs.

In 587 hospitalised children, 26 (4.4%) HCoVs were identified, and 2.6% were HCoV-NL63.[5] The peak season for infection was in spring and summer of 2002. In 2004/2005, HCoVs were found in 2.1% of adults and children hospitalised for acute RTIs, with HCoV-NL63 accounting for 0.4%.[4] Both HCoV-HKU1 and HCoV-OC43 infections peaked in winter, whereas HCoV-NL63 infections occurred mainly in early summer and autumn. In the present study, 74 (2.5%) patients were detected to have HCoV infection in 2005 to 2007. The seasonality pattern for HCoV-NL63 was consistent with another study (Fig).[4] Interestingly, the detection rates of HCoV-NL63 were significantly different in the two 12-month periods (Table 1). Thus, studies that look for HCoV-NL63 in any 1-year period only might produce inaccurate epidemiological results.[5]

CoV, being an RNA virus, has a high degree of genetic diversity. Phylogenetic analyses of 1a and spike gene sequences revealed that most circulating HCoV-NL63 were closely related to strains in Netherlands (NL72 and NL496) and Belgium (BE03 1153, BE03 64880).[5] A small proportion of the strains circulating in Hong Kong were phylogenetically distinct from the major group.[1,2] We suggest including representative samples from both clusters of isolates when evaluating diagnostic assays.

Acknowledgements

References

1. Fouchier RA, Hartwig NG, Bestebroer TM, et al. A previously undescribed coronavirus associated with respiratory disease in humans. Proc Natl Acad Sci U S A 2004;101:6212-6.
2. van der Hoek L, Pyrc K, Jebbink MF, et al. Identification of a new human coronavirus. Nat Med 2004;10:368-73.
3. Moes E, Vijgen L, Keyaerts E, et al. A novel pancoronavirus RT-PCR assay: frequent detection human coronavirus NL63 in children hospitalized with respiratory tract infections in Belgium. BMC Infect Dis 2005;5:6.
4. Lau SK, Woo PC, Yip CC, et al. Coronavirus HKU1 and other coronavirus infections in Hong Kong. J Clin Microbiol 2006;44:2063-71.
5. Chiu SS, Chan KH, Chu KW, et al. Human coronavirus NL63 infection and other coronavirus infections in children hospitalized with acute respiratory disease in Hong Kong, China. Clin Infect Dis 2005;40:1721-9.

M Jaume
MS Yip 葉名琛
YW Kam 甘曜榮
CY Cheung 張頌恩
F Kien
A Roberts
PH Li 李炳雄
I Dutry
N Escriou
M Daeron
R Bruzzone
K Subbarao
JSM Peiris 裴偉士
B Nal
R Altmeyer

Key Messages

1. A SARS vaccine was produced based on recombinant native full-length Spike-protein trimers (triSpike) and efficient establishment of a vaccination procedure in rodents.
2. Antibody-mediated enhancement of SARS-CoV infection with anti-SARS-CoV Spike immune-serum was observed in vitro.
3. Antibody-mediated infection of SARS-CoV triggers entry into human haematopoietic cells via an FcγR-dependent and ACE2-, pH-, cysteine-protease-independent pathways.
4. The antibody-mediated enhancement phenomenon is not a mandatory component of the humoral immune response elicited by SARS vaccines, as pure neutralising antibody only could be obtained.
5. Occurrence of immune-mediated enhancement of SARS-CoV infection raises safety concerns regarding the use of SARS-CoV vaccine in humans and enables new ways to investigate SARS pathogenesis (tropism and immune response deregulation).

HKU-Pasteur Research Centre
M Jaume, MS Yip, YW Kam, F Kien, PH Li, I Dutry, R Bruzzone, JSM Peiris, B Nal
Department of Microbiology, The University of Hong Kong
CY Cheung, JSM Peiris
Laboratory of Infectious Diseases, NIAID, National Institutes of Health, Bethesda, USA
A Roberts, K Subbarao
Institut Pasteur, Unite de Genetique Moleculaire des Virus Respiratoires, Paris, France
N Escriou
Institut Pasteur, Departement d'Immunologie, Unite d'Allergologie Moleculaire et Cellulaire, Paris, France
M Daeron
CombinatoRx-Singapore Pte Ltd, Singapore
R Altmeyer

RFCID project number: 05050182

Principal applicant:
Beatrice Nal
HKU-Pasteur Research Centre, 8 Sassoon Road, Hong Kong SAR, China
Tel: (852) 2816 8422
Fax: (852) 2872 5782
Email: bnal@hku.hk

Corresponding author:
Martial Jaume
HKU-Pasteur Research Centre, 8 Sassoon Road, Hong Kong SAR, China
Tel: (852) 2816 8423
Fax: (852) 2872 5782
Email: breizh@hku.hk

SARS CoV subunit vaccine: antibody-mediated neutralisation and enhancement

Introduction

Public health measures successfully contained outbreaks of the severe acute respiratory syndrome coronavirus (SARS-CoV), which infected more than 8000 people worldwide with a mortality of about 10%. However, concerns over future recurrences remain. Continuous efforts have been made to develop safe vaccine strategies against SARS-CoV.

Among the four major structural SARS-CoV proteins, the Spike envelope glycoprotein (S) is the most significant SARS-CoV neutralising and protective antigen. The binding of the Spike protein to its receptor Angiotensin Converting Enzyme 2 (ACE2) is responsible for SARS-CoV entry into cells. Vaccine strategies aiming at blocking/restricting infection by SARS-CoV mainly focus on targeting the Spike viral glycoprotein. Nonetheless, such strategy poses a singular dilemma for coronaviruses, as previous vaccination protocols have highlighted the possibility of immune-mediated enhancement of the disease.[1,2]

Immune-mediated mechanisms, particularly antibody-dependent enhancement (ADE) have been exploited by a variety of viruses, including dengue virus, Feline Coronavirus (FCoV), and HIV, as alternative strategies to infect host cells.[2,3] Besides interaction between viral protein and host receptor, these viruses can enter cells through binding of virus/immune-complexes to Fc-receptor (FcR), complement-receptor or by inducing conformational change in envelope glycoproteins that are required for virus-cell membrane fusion.[3] In the case of FcoV infection, immunisation of cats with recombinant vaccinia virus preparations expressing the FCoV Spike protein resulted in the induction of S-specific antibodies responsible for an enhanced susceptibility to infectious challenge.[1] The enhanced infection of macrophages following antibody-mediated entry of feline coronavirus is responsible for the occurrence of deadly feline infectious peritonitis.

We investigated whether a recombinant native full length Spike-protein trimer (triSpike) of SARS-CoV was able to elicit a neutralising and protective immune response. Furthermore, we explored the capacity of vaccine-induced anti-Spike immune-serum to mediate ADE of SARS-CoV infection. We adopted reasonable safety concerns regarding the use of SARS-CoV vaccine in humans, and explored new ways to investigate SARS pathogenesis.

Methods

This study was conducted from 17 July 2006 to 16 June 2008.

Cell lines, expression vectors

VeroE6 (African green monkey kidney epithelial cells), K-562 (human chronic myelogenous leukaemia cells), U-937 (human histiocytic lymphoma cells), THP-1 (human acute monocytic leukaemia cells), SUP-T1 (human lymphoblastic leukaemia T lymphoblast), MOLT-3 (human acute lymphoblastic leukaemia T lymphoblast), MT4/R5 (Human T cell lymphoblast expressing CCR5), Raji (Burkitt's lymphoma B lymphoblast), Daudi (Burkitt's lymphoma B lymphoblast), ST486 (Burkitt's lymphoma B lymphoblast lacking expression

of FcγR), 721.221 (EBV-transfected human B cells), NK-92 (malignant non-Hodgkin's lymphoma NK cell), P388D1 (murine macrophage-like lymphoblast), J774A.1 (murine monocyte/macrophage cells) were cultured in accordance with ATCC guidelines. Optimised DNA and Semliki Forest Virus expression vectors encoding SARS-CoV S-protein fused to a C-terminal FLAG-sequence have been described.[4]

Immunisation with inactivated SARS-CoV or recombinant Spike protein

For evaluation of ADE of triSpike-elicited serum, BALB/c mice 6 to 8 weeks old (n=4 per group) were immunised intraperitoneally with 2 µg of purified triSpike in presence or absence of 1 mg of aluminium hydroxide gel on days 0 and 28. Animals in the control group received PBS with 1 mg of aluminium hydroxide gel on the same days. Blood samples were collected by saphenous vein bleeding on days -1, 27 and 55 post-immunisation (in accordance with local guidelines), and sera were prepared and heat-inactivated.

For comparison of SARS-CoV vaccines, BALB/c mice (n=4 per group) were immunised intraperitoneally with either 2 µg of recombinant codon-optimised SARS-CoV Spike full-length (Opt. Spike Flag; O.S.F; aa1-1255), 2 µg of recombinant codon-optimised SARS-CoV Spike ectodomain (Opt. SpikeECD Flag; O.SECD.F; aa1-1184), 2 µg of recombinant codon-optimised SARS-CoV Spike subunit 1 (Opt. S1 Flag; O.S1.F; aa1-757), or 10 µg of recombinant SARS-CoV Spike protein truncated early after the transmembrane domain (Soluble Spike Flag; Ssol.F; aa1-1193). An additional group immunised with 2 µg (Spike-equivalent) of γ-irradiated SARS-CoV virion was also included as well as a mock control group injected with saline solution (PBS). Two immunisations were performed in presence of 1 mg of aluminium hydroxide gel at 3-week intervals, and sera were collected on days -1, 27, and 55 post-immunisation. Blood samples were harvested and handled as described above.

SARS-CoV pseudotype particles

Recombinant SARS-CoVpp lentiviral vectors expressing a luciferase reporter gene were produced from HEK293T cells as described elsewhere using 10 µg of plasmid pNL4.3.Luc R–E–pro– and 10 µg of plasmid pCDNA-S-FLAG encoding codon-optimised SARS-CoV S protein.[4] For ADE assays, 25 µL of serial two-fold dilutions of heat-inactivated mouse sera were incubated for 1 h at 37°C with 25 µL of pseudovirus (50 ng p24). 50µL of Raji cells, at 2×10^6 cell/mL previously washed three times with serum-free RPMI, were added to the antibody-SARS-CoVpp mixture in a 96-well plate. After adsorption for 1 h at 37°C, 100 µL of RPMI 1640 containing 5% FCS were added. Medium was renewed 16 h later and cells were incubated for an additional 48 h, washed in PBS, lysed and luciferase activity measured for 10 sec in a MicroBeta Jet Counter (Perkin Elmer) according to the instructions provided by the supplier (Promega). For ADE blocking assays, Raji cells were pre-incubated for 15 min at 4°C with 10 µg/mL of murine monoclonal antibody directed against human CD32 (FcγRII, BD Pharmingen) or goat polyclonal antibody directed against human ACE2 (R&D Systems) prior to infection with SARS-CoVpp.

Lysosomotropic agent and protease inhibitors

Cells were pre-incubated with the indicated amounts of either ammonium chloride (NH_4Cl) for 1 h, E-64d or Cathepsin L inhibitor (Cat L Inh) (Calbiochem) for 3 h prior to infection. Pseudoviruses (with or without serum) were mixed with the same concentrations of reagents in tubes and added to cells. After 5 h (E-64d or Cat L Inh) or 7 h (NH_4Cl), viruses were removed and replaced with fresh medium without drug. Cells were assayed for luciferase activity 60 to 65 h after infection.

Results

Production of a subunit SARS vaccine

We developed a SARS vaccine candidate (triSpike) based on recombinant native full-length Spike-protein trimers (the envelope glycoprotein involved in SARS-CoV entry into host cells). Our vaccine protocol elicited an in vivo neutralising and protective immune response in rodents.[4] In vitro Spike-specific serum blocked binding of the Spike protein to the ACE2 receptor and neutralised SARS-CoV infection of permissive cells.[4]

### Investigation of immune-mediated enhancement of SARS-CoV infection

By using SARS-CoV Spike-pseudotyped viral particle (SARS-CoVpp),[4] we analysed the capacity of triSpike-elicited sera to trigger ADE[2,3] of viral infection in vitro. The experiments exhibited opposite pattern according to cell types, while complement-inactivated sera from immunised animals still inhibit SARS-CoVpp entry in prototypic permissive cell lines, these sera induced virus penetration in human monocytic and lymphoblastic (B lineage) cell lines (Fig 1). Immune-mediated enhancement of infection was not restricted only to SARS-CoVpp, but also drove infection of human Raji B cells by live SARS-CoV (strain HK39849).

Unravelling molecular and biochemical pathways of antibody-dependent enhancement of SARS-CoV infection

To highlight differences, if any, in the ACE2[5] and FcR-mediated entry pathways, we compared the effect of treatments by a lysosomotropic agent and protease inhibitors. Blockade of the acidification of the endosome, and annihilation of the cysteine protease activity did not abrogate ADE of SARS-CoVpp infection (Fig 2). In combination with the results of the investigation of the molecular pathway involved during the ADE process, entry into human haematopoietic cells occurred via an FcγR-dependent[4] and ACE2-, pH-, cysteine-protease-independent[4] pathways illustrating that ADE of virus infection is a novel cell entry mechanism of SARS-CoV (Fig 2).
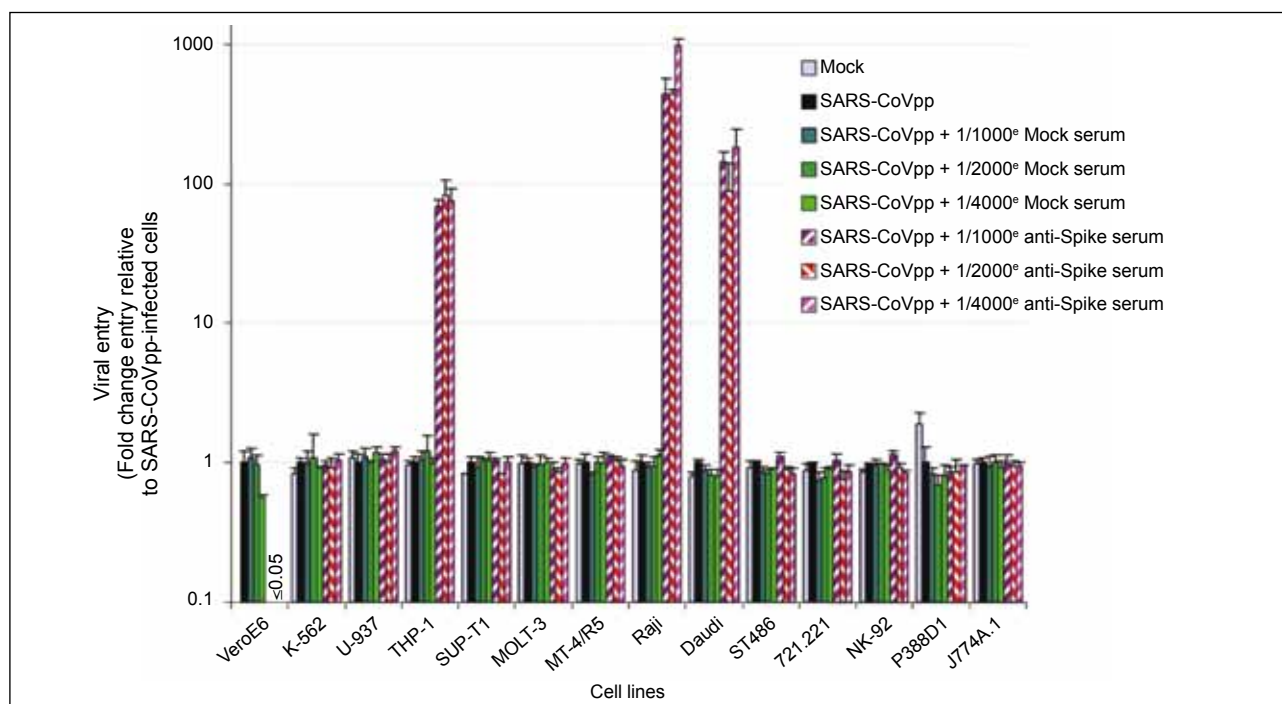
Fig 1. Susceptibility of haematopoietic cell lines to infection by SARS-CoV Spike pseudoparticles in presence of immune-serum
SARS-CoVpp were incubated in presence or absence of different dilutions (eg 1/1000, 1/2000, and 1/4000) of serum from PBS/Alum-immunised (plain bars) or 2 μg triSpike/Alum-immunised (hatched bars) BALB/c mice for 1 h prior to addition to the indicated cells. Three days post infection, 1 volume of luciferase substrate reagent was added to wells and luminescence was measured (Figure amended with permission from the *American Society for Microbiology* from FIG. 1A of the original publication[6])
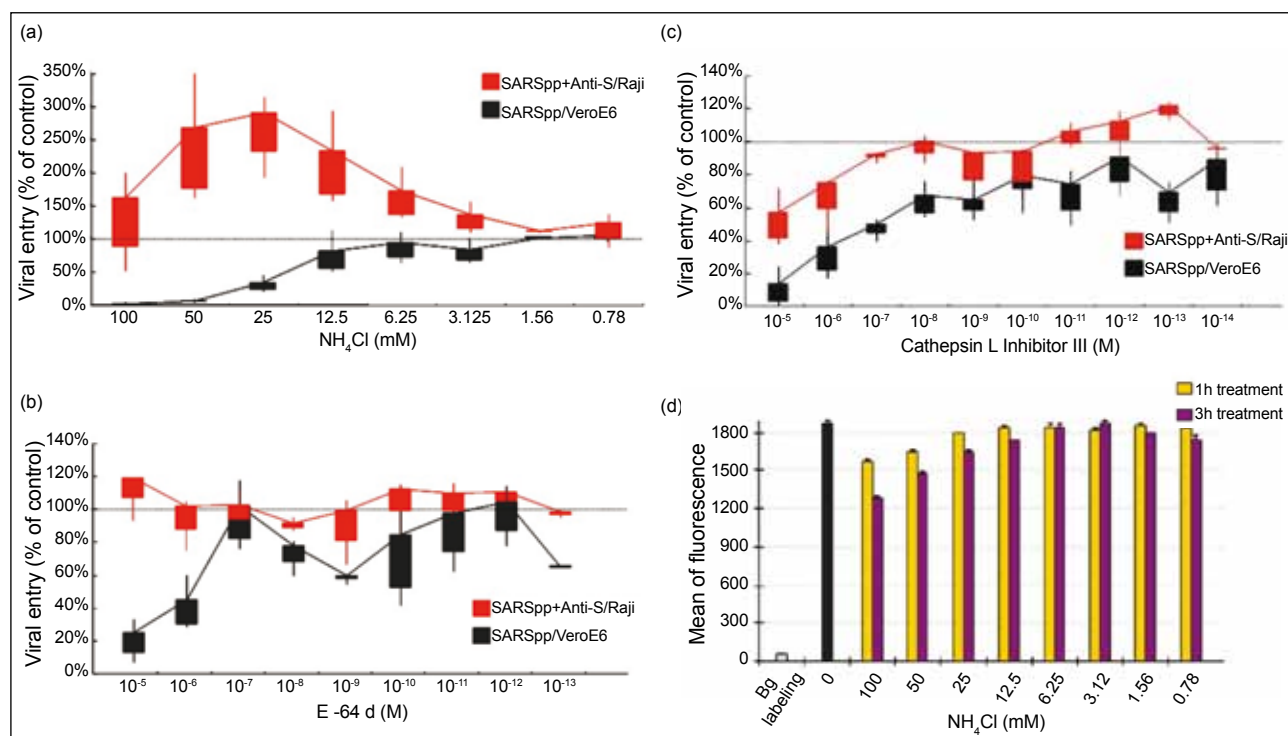
Fig 2. Antibody-mediated entry of SARS-CoVpp is independent of acidic pH and cysteine-protease activity of the endosomal/lysosomal compartment
Comparison of pH and protease requirements for ACE2- versus antibody-mediated entry of SARS-CoVpp. Prior to infection, VeroE6 and Raji cells were preincubated with indicated concentration of (a) ammonium chloride (NH_4Cl) for 1 h or (b) broad cysteine proteases inhibitor (E-64d) or (c) Cathepsin L inhibitor (Cat L Inh) for 3 h. SARS-CoVpp ± 1/2000 anti-Spike serum (containing the indicated concentration of chemicals) was then added to the cells. (d) Cell surface expression of hCD32 protein on Raji cells following NH_4Cl treatment. Raji cells were incubated with indicated concentrations of NH_4Cl for 1, 3, and 5 h (not shown). Cells were then labelled with anti-hCD32 antibody and subjected to flow cytometry (Figure amended with permission from the *American Society for Microbiology* from FIG. 7 of the original publication[6])
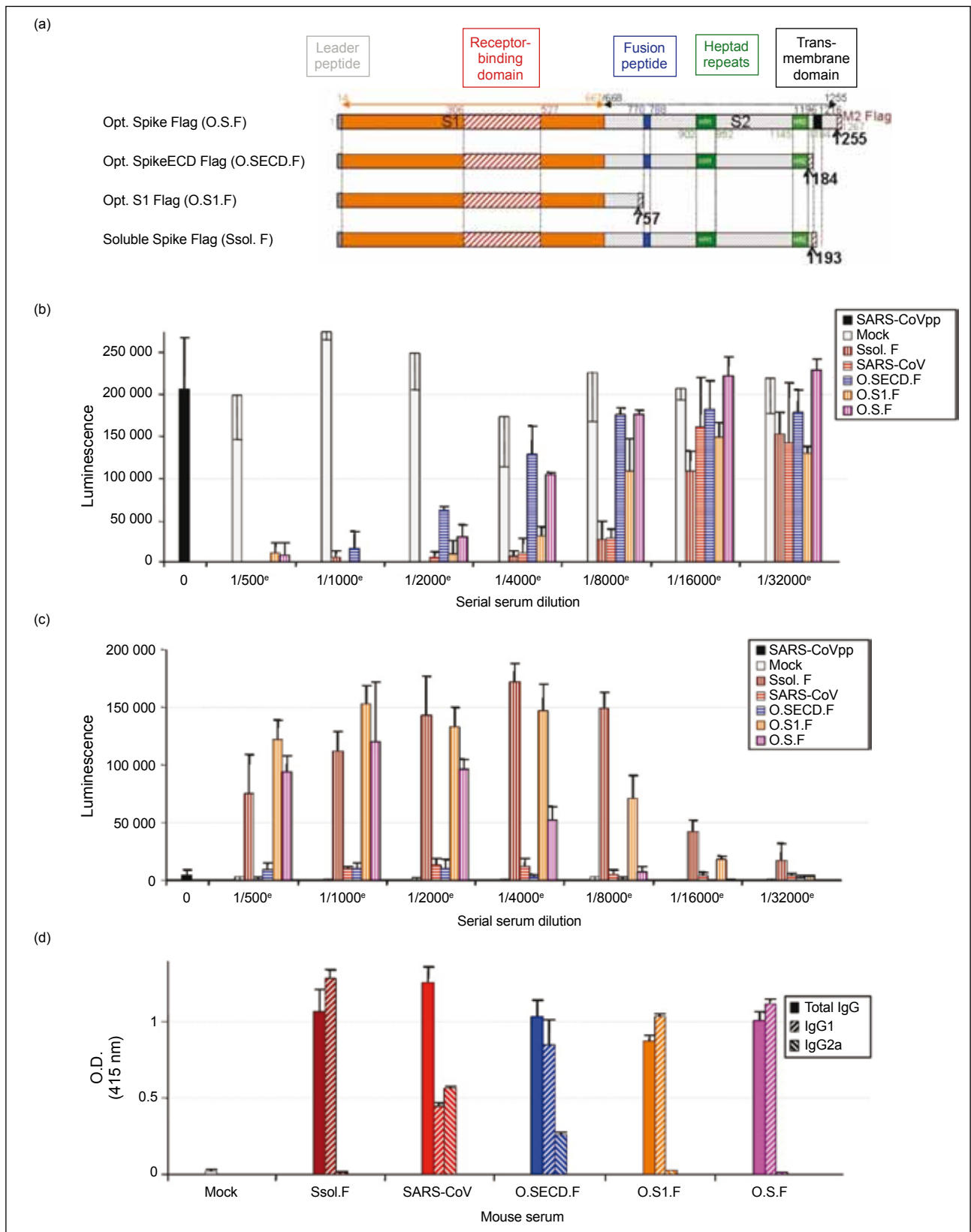
Fig 3. Effect of different vaccine formulation on SARS-CoV antibody-mediated enhancement of viral entry
Schematic illustration of different forms of recombinant SARS-CoV Spike used for vaccination of BALB/c mice. (a) Positions of the different regions are indicated according to Swissprot accession no. P59594. Neutralising versus enhancing abilities of mouse sera raised after immunisation with different SARS vaccine candidates are shown. SARS-CoVpp were incubated in presence or absence of serial dilutions of pooled serum from four vaccinated BALB/c mice as indicated for 1 h prior to addition to the (b) VeroE6 or (c) Raji cells. Three days post-infection luminescence was measured. (d) The binding activity toward recombinant SARS-CoV Spike protein in 1/2000 dilution of pooled serum from vaccinated mice was estimated by enzyme-linked immune-absorbent assay (Figure amended with permission from the *American Society for Microbiology* from FIG. 8 of the original publication[6])

SARS vaccine candidates and antibody-dependent enhancement of SARS-CoV infection

By comparing neutralising versus enhancing potency of different SARS vaccine candidates (subunit vaccines and whole inactivated virion), distinct patterns of ADE were highlighted, despite highly similar abilities of the immune-sera to neutralise infection of ACE2-expressing cells (Fig 3). Noticeably, two out of the five tested immunogens (Spike ectodomain only and whole inactivated virion) displayed relatively high neutralising titres without triggering SARS-CoVpp entry into immune cells. Preliminary results showed differences in the nature of humoral responses elicited by the five immunogens, as indicated by presence or absence of IgG2a in non-enhancing and enhancing sera, respectively (Fig 3).

Discussion

Currently, there is no licensed vaccine against a human coronavirus. Nonetheless, vaccines against some animal coronaviruses have been generated. Other vaccines are difficult to produce owing to immune enhancement of infection.[1,2]

Our quest to produce an efficient vaccine against SARS-CoV has shed light on the incidence of opposite outcomes (ie neutralising and enhancing) depending on the patterns of expression of Fc receptor by the host cells. Notably, occurrence of antibody-mediated infection seems fairly complex as the expression of a particular class of FcR is not sufficient to indubitably predict the occurrence of ADE. Indeed, only background levels of SARS-CoVpp transduction were observed with several immune cells (human K-562, MT4-R5, 721.221, and murine P388D1, J774A.1 cell lines) despite their expression of the same FcγR (FcγRII) as THP-1, Raji, and Daudi cells (Fig 1). The reasons for this phenomenon remain unclear, but the involvement of FcR subfamilies, such as activating and inhibiting isoforms (ITAM- and ITIM-bearing FcR, respectively) and/or allelic variants, ie FcRγIIA-H131 and FcRγIIA-R131, is highly speculative.

Our studies on the biochemical requirements along the antibody-mediated infection have proved this pathway singularly distinct from the natural (ie ACE2) entry mechanism. In fact, ADE of SARS-CoVpp entry into human haematopoietic cells occurred via an ACE2-, pH- and cysteine-protease-independent route, illustrating that antibody-mediated infection is a novel cell entry mechanism of SARS-CoV.

Investigation of the neutralising versus enhancing potency of immune-sera elicited by different SARS vaccine candidates have highlighted distinct patterns of ADE, despite highly similar abilities to neutralise SARS-CoV infection. Further studies of the mechanisms underlying ADE of SARS-CoV infection are needed, particularly to unravel which viral epitope(s) or immunoglobulin isotype(s) are responsible for the enhanced infection.

Because of antibody-mediated infection of SARS-CoV, we hypothesised that the ADE phenomenon might participate in SARS pathogenesis. Indeed, infection by SARS-CoV is not confined to the lungs, but also involves other organs, most importantly cells of the immune system. Direct infection of haematopoietic cells by SARS-CoV may provide a partial explanation for the widespread destruction of the lymphoid tissue and the cytokinic deregulation in many SARS patients. Nonetheless, it is not clear how SARS-CoV gets a foothold into the immune cells as they do not express the putative SARS-CoV receptor ACE-2. Antibody-dependent enhancement of SARS-CoV infection, in addition to other alternative entry pathways (involving C-type lectin), may provide SARS-CoV versatility in entry routes allowing it to broaden its target options.

Acknowledgements

References

1. Vennema H, de Groot RJ, Harbour DA, et al. Early death after feline infectious peritonitis virus challenge due to recombinant vaccinia virus immunization. J Virol 1990;64:1407-9.
2. Huisman W, Martina BE, Rimmelzwaan GF, Gruters RA, Osterhaus AD. Vaccine-induced enhancement of viral infections. Vaccine 2009;27:505-12.
3. Sullivan NJ. Antibody-mediated enhancement of viral disease. Curr Top Microbiol Immunol 2001;260:145-69.
4. Kam YW, Kien F, Roberts A, et al. Antibodies against trimeric S

glycoprotein protect hamsters against SARS-CoV challenge despite their capacity to mediate FcgammaRII-dependent entry into B cells in vitro. Vaccine 2007;25:729-40.

5. Huang IC, Bosch BJ, Li F, et al. SARS coronavirus, but not human coronavirus NL63, utilizes cathepsin L to infect ACE2-expressing cells. J Biol Chem 2006;281:3198-203.

6. Jaume M, Yip MS, Cheung CY, et al. Anti-severe acute respiratory syndrome coronavirus spike antibodies trigger infection of human immune cells via a pH- and cysteine protease-independent FcγR pathway. J Virol 2011;85:10582-97.

S Riley
GM Leung 梁卓偉
BJ Cowling 高本恩

Key Messages

1. The ability to detect and differentiate between fast and slow spatial spread of infectious disease depends on the density of the surveillance network.
2. The results of this study suggest that more concentrated surveillance networks are required in Guangzhou compared with other regions, such as Thailand and Europe, as long-distance travel is less frequent.

Department of Community Medicine and School of Public Health, The University of Hong Kong
S Riley, GM Leung, BJ Cowling

RFCID project number: 05050122

Principal applicant and corresponding author:
Dr BJ Cowling
Department of Community Medicine,
School of Public Health, The University of Hong Kong, Unit 624-627, Level 6, Core F, Cyberport 3, 100 Cyberport Road, Hong Kong SAR, China
Tel: (852) 3906 2011
Fax: (852) 3520 1945
Email: bcowling@hku.hk

Public health interventions to control the spread of a directly transmitted human pathogen within and between Hong Kong and Guangzhou

Background

The 2003 outbreak of severe acute respiratory syndrome (SARS) highlighted the social connectivity between mainland Chinese cities and Hong Kong. Epidemiological and molecular analyses suggest that the Hong Kong outbreak was seeded from Guangzhou. In future outbreaks of new or re-emerging directly transmitted infectious diseases, it would be desirable to quantify the pathogen-specific risk of transmission between these two city populations, based on the natural history of the disease and a detailed contact model of the populations involved.

Large-scale transmission models provide a versatile experimental structure for infectious disease epidemiology. Each host is usually represented explicitly in the model and is assigned a location in space. Typically, nodes may be susceptible, exposed but not yet infectious, infectious, or recovered. Infections occur either along arcs in the network or according to a spatial infection kernel. These models are used to investigate how patterns of spread are changed by public health interventions.

Properties of the network and transmission kernel are usually determined by surveillance data on how people travel to work. Reliable travel data are required to correctly parameterise large-scale transmission models. Previous modelling studies have used census-derived data to parameterise human movement. As part of an integrated study, we conducted a bespoke telephone questionnaire in order to generate data specific to our study population.

Methods

This study was conducted from 1 October 2006 to 29 February 2008. A household-based telephone survey was conducted using random digit dialling in the metropolitan areas of Guangzhou, Foshan, and Hong Kong. The interviewer asked the respondent for the district in which the household was located, how many people lived in the household, and if anyone in the household had owned poultry in the past month. The next section of the questionnaire was on an individual basis. The respondent was asked to answer on behalf of any household members who were not present.

The origin and destination locations for each respondent (as described above) and fine-resolution population density estimates from the Landscan model of human population density was used to estimate a pair-wise choice kernel for each city within the survey. A static network model of an infectious disease outbreak of a novel respiratory pathogen was constructed and the model was parameterised using data from the travel questionnaire.

Results

A total of 3318 households completed the questionnaires: 906 in Foshan, 1819 in Guangzhou, and 593 in Hong Kong. The total number of individuals was 3349 in

Foshan, 5991 in Guangzhou, and 1854 in Hong Kong. The mean size of households was 3.7 persons in Foshan, 3.3 in Guangzhou, and 3.1 in Hong Kong.

An outbreak of pandemic influenza was simulated over the derived network, seeded within 10 km of the centre of Guangzhou. Due to the short generation time of pandemic influenza, the progression of the outbreak was rapid. For an outbreak seeded in Guangzhou, using the data from our telephone survey, local transmission dominated and no significant outbreaks were observed in nearby highly populated areas. This pattern contrasts sharply with predicted spatio-temporal dynamics for influenza in Thailand and Europe.

Conclusions

A slower spatial spread of influenza in southern China has public health implications, particularly for containment and surveillance. The slower the spatial spread for a given number of cases, the greater the requirement for surveillance. If the infection spreads rapidly, there is a much greater chance that it will be picked up by a sparse surveillance network. However, if the disease spreads slowly, then the number of cases that will occur before the disease appears on a sparse surveillance network will be much higher. Therefore, our results suggest that the surveillance network in China should be more intensive than in Thailand.

Acknowledgement

J Niu 牛建磊
CW Tung 董志華
N Gao 高乃平

Inter-flat airflow and airborne disease transmission in high-rise residential buildingsz

Key Messages

1. A virus-spread mechanism is related to inter-flat or inter-zonal airflow through open windows caused by buoyancy effects.
2. Both on-site measurements and numerical simulations quantify the amount of the exhaust air that exits the upper part of the window of a floor and re-enters the lower part of the open window of the immediately upper floor.
3. Ventilation air could contain up to 7% (in terms of mass fraction) of the exhaust air from the lower floor.
4. In high-rise buildings, windows flush with the facade are a major route for the vertical spread of pathogen-containing aerosols, especially those <1 µm in diameter.

Department of Building Services Engineering, The Hong Kong Polytechnic University
J Niu, CW Tung, N Gao

RFCID project number: 03040642

Principal applicant and corresponding author:
Dr Niu Jianlei
Department of Building Services Engineering, The Hong Kong Polytechnic University, Hung Hom, Kowloon, Hong Kong SAR, China
Tel: (852) 2766 4698
Fax: (852) 2774 6146
Email: bejlniu@polyu.edu.hk

Introduction

The outbreak of the severe acute respiratory syndrome (SARS) in 2003 called for closer investigation of the possible transmission routes of infectious diseases in the environment. There were SARS clusters in several high-rise residential blocks in Hong Kong,[1] at Koway Court (Chai Wan) on 25 March 2003, Hing Tung House (Tung Tau (II) Estate, Kowloon City) on 2 April 2003, and Wing Shui House (Lek Yuen Estate, Shatin) on 7 May 2003. Most of the affected households were located along the same vertical block on different floors. The possibility of spread via unsealed U-traps of the drainage systems was ruled out. Especially in the case of Wing Shui House, SARS coronavirus was found in swab samples collected from the wall, windows, and the floors of two units near the index unit, while the residents of these two units had no symptoms of the disease.[1] The vertical spread of the disease suggested that it had been transmitted via airflow under certain environmental conditions.

This study aimed to confirm whether the inter-flat airflow can form a significant path for residents to become exposed to virus-containing aerosols generated by an index patient via sneezing, coughing, and speaking in the flat below. Airflow through open windows was focused, particularly in Wing Shui Building, Shatin, which had single-sided natural ventilation.

Methods

This study was conducted from 1 December 2005 to 30 April 2007. The airborne disease transmission path was investigated using on-site ventilation and tracer gas measurements, as well as computer simulations of the airflow and residual droplet movements.

For on-site measurements of cross contamination of ventilation, three buildings were selected. In each building, two vertically adjacent flats were rented for about one month for tracer gas and ventilation measurements. Two tracer gases SF_6 and CO_2 were used simultaneously to examine contaminant dispersion and ventilation rates of the two selected rooms. SF_6 was used both as a tracer of indoor pollutants originating from the lower floor and for the calculation of air change rate in the lower floor room, and CO_2 merely as tracer for determining the ventilation rates. The SF6 concentrations at six different points within the two rooms were continuously monitored (Fig).

A computational fluid dynamics program solves the governing equations of airflow field in a finite-volume procedure with a staggered grid system. The turbulent effect of flows is simulated by the re-normalisation group k-ε model. The dispersion of gaseous pollutants can be simulated by solving the governing equation of species in air. Since human-generated aerosols mainly range from 1 to 1000 µm in diameter, a relatively large discrepancy may appear for coarse particles whose gravitational settling effect is remarkable. In order to look into the movement of the pathogen-containing droplets, the cascade transport of pollutants in the form of particles was simulated by both Eulerian and Lagrangian methods, as validated in our earlier publication.[2]

Results and discussion

The mean SF_6 concentrations of the six monitored points were arranged in descending order as 1.31×10^5, 5.94×10^4, 4.88×10^4, 2.83×10^3, 2.05×10^3, and 1.37×10^3 µg m^{-3}, at points P-3, P-2, P-1, P-4, P-5, and P-6, respectively (Fig). The highest concentration was found at P-3, which represented the source point of the index room. The concentrations at P-1 and P-2, close to the source point, were of the same order of magnitude, with P-2 being slightly higher than P-1. This was related to the route of the airflow. P-2 was at the upper part of the window, which was the outlet of the infected airflow due to buoyancy forces. Fresh air came into the room via P-1, which mixed with the contaminated air, and exhausted through P-2. The concentrations in the upper room at P-4, P-5, and P-6 were much lower than those in the source room at P-1, P-2, and P-3. This indicated that the consecutive dilutions took place along the airflow path during the transmission.

To further quantify this potential inter-flat airflow, two indices were defined based upon a three-zone airflow and a mass balance model. The mass fraction M_{i-j} was defined as the mass fraction of air that originated from the point i in the lower source room and was present in the point j of the upper room. By assuming a quasi-steady airflow process, the mass fraction M_{i-j} can be directly calculated from the monitored tracer gas concentrations using equation 1:

$$M_{i-j} = \frac{Cj}{Ci},$$

where Ci and Cj were the monitored tracer gas concentrations in the source room and the secondary room. Another index, the re-entry ratio k, was defined as the fraction of the exhaust air from the lower source room which re-entered the adjacent/upper room. By assuming a steady state airflow and mixing process and well mixed conditions for both rooms, the re-entry ratio k can be calculated using equation 2:

$$k = M_{i-j} \ \frac{V_2(ACH)_2}{V_1(ACH)_1},$$

where V_1 and V_2 were the room volumes and $(ACH)_1$ and $(ACH)_2$ the measured air change rates (hr^{-1}).

As far as the spread of infectious disease is concerned, the index mass fraction M_{i-j} may be the more direct index. As an extension of the well-mixed assumption, two local mass fractions, M_{2-4} (the fraction of air present at P-4 and originating from P-2) and M_{2-6} (the fraction of air present P-6 and originating from P-2) were calculated from equation 1 (Table 1). The value of M_{2-4} was larger than M_{2-6}, as P-6 was further away from the source. Hence, P-6 had more dilution than P-4, as described in the previous section. The maximum mass fraction M_{2-4} was about 0.07, which meant that the air near the window upstairs contained 7% of the exhaust air originating from the lower room. The current ASHRAE ventilation standard[3] promulgates that the dilution factor should exceed the value 50 to 1 when highly hazardous pollutants are involved, which would correspond to the mass fraction round 0.02.[3] Increasing wind speed was shown to suppress the value of the mass fraction. At a low wind speed of 0.03 m/s, the mass fractions at the two points in the upper room reached to values of M_{2-4}=0.07, M_{2-6}=0.029, respectively. When the wind speed was at the higher end (0.87 m/s), the mass fractions were reduced to M_{2-4}=0.04, M_{2-6}=0.016. At both low wind and small indoor-outdoor temperature differences, the mass fraction tended to be higher, which agreed with our hypothesis that pure but low buoyancy driven flow on calm days may pose the highest infection risks.
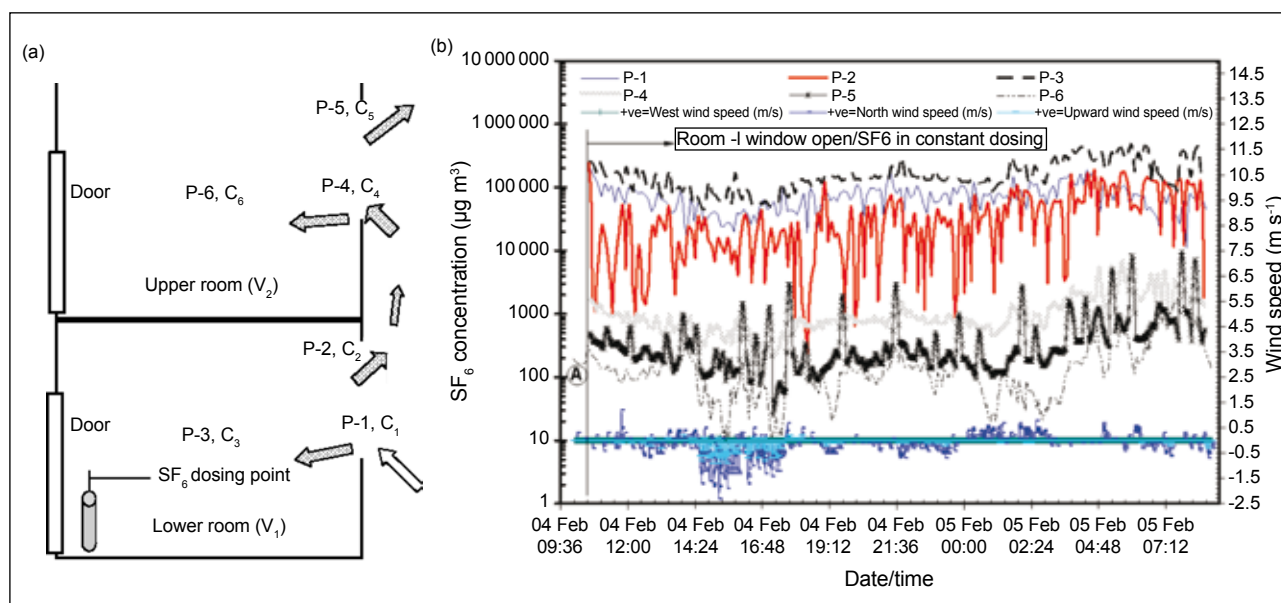

Fig. (a) Tracer-gas dosing and sampling points in the two adjacent floors upstairs and downstairs. (b) Example concentration profiles of tracer gas SF_6 at the six points on two low-wind days

Table 1. Mass (M) fractions, ratio of air change rates per hour (ACH) of the two rooms, re-entry ratio of exhaust air at different wind ranges

Wind speed (m/s)	M_{2-4}	M_{2-6}	$(ACH_1)/(ACH_2)$	Re-entry ratio k	No. of data set
≤0.03	0.070	0.029	1.64	0.048	4740
0.25	0.055	0.026	1.71	0.044	2080
0.45	0.050	0.022	1.73	0.038	1306
0.66	0.046	0.019	1.74	0.033	653
0.87	0.041	0.016	1.75	0.028	270
1.07	0.039	0.011	1.69	0.019	135
1.3	0.038	0.006	1.66	0.01	82
1.5	0.032	0.007	1.65	0.011	46
1.69	0.035	0.005	1.67	0.009	43
1.88	0.038	0.005	1.61	0.009	32
2.11	0.033	0.005	1.64	0.008	19
2.48	0.036	0.004	1.75	0.006	

Numerical simulations

Based on the knowledge of infection dose (the number of organisms required to cause infection), the risk of airborne infection and ventilation rate per person can be correlated by the Wells-Riley equation.[4] Assume that one patient standing at the middle of the second floor producing 13 infectious quanta per hour, pulmonary ventilation rate to be 0.6 m^3/h, and exposure time of 8 hours, the calculated mean infection probabilities can be as high as 6.6% on the third floor (Table 2).

The upper to lower concentration ratio for 1.0 μm particles was close to the values for CO_2. The results of 10.0 and 20.0 μm particles differed from the 1.0 μm particle remarkably. Different from gaseous pollutants, two factors constrained the cascade effect of coarse particles: (1) the effect of gravity on the particles which counteracts the upward buoyancy force, and (2) the absorption of particles on solid surfaces. The latter is a self-cleaning mechanism of particles, which contributes to decreasing suspended concentrations in the lower floor and reducing outlet concentrations.

Conclusions

On-site airflow visualisation, tracer gas measurements, and numerical simulations revealed qualitatively and quantitatively the vertical upward re-entry possibilities of the exhaust air in high-rise residential buildings by open window ventilation practices. The presence of exhaust air from a lower room in an adjacent upper room can reach up to 7%, in terms of mass fraction. With regard to the transmission risk from a lower floor to the floor

Table 2. Mean risk of infection calculated from the Wells-Riley equation (based upon 8-hour exposure, using *Mycobacterium tuberculosis* as the pathogen)

Mean risk of infection on	Infection probability at wind speed of				
	0.1 m/s	0.5 m/s	1.0 m/s	2.0 m/s	4.0 m/s
Second floor	30%	28%	29%	31%	46%
Third floor	2.0%	3.4%	3.5%	6.6%	1.7%

immediately above via this route, the order is one magnitude lower than the risk in the same household. But this risk should not be overlooked. As one of the effective intervention measures is to isolate and quarantine the close-contacts, the upstairs household residents may be included in the close-contact list in the event of a highly infectious disease.

Acknowledgement

References

1. Hong Kong Health Welfare & Food Bureau. SARS Bulletin-28 May 2003, Available at http://www.info.gov.hk/dh/diseases/ap/eng/bulletin0528e.pdf. Accessed 10 November 2004.
2. Gao NP, Niu JL. Modelling particle dispersion and deposition in indoor environments. Atmospheric environment 2007;41:3862-76.
3. American Society of Heating, Refrigerating and Air-Conditioning Engineers. ANSI/ ASHRAE 62. Ventilation for acceptable indoor air quality. Atlanta: American Society of Heating, Refrigerating and Air-Conditioning Engineers; 2004.
4. Riley EC, Murphy G, Riley RL. Airborne spread of measles in a suburban elementary school. Am J Epidemiol 1978;107:421-32.

SY Yik 易雪怡
MS Yu 余雯珊
YS Ho 何宛姍
CSW Lai 賴秀芸
YT Cheung 張婉婷
KF So 蘇國輝
RCC Chang 鄭傳忠

Neuroprotective effects of minocycline on double-stranded RNA-induced neurotoxicity in cultured cortical neuronsz

Key Messages

1. Minocycline, memantine, and glycoconjugate were assessed for their ability to protect cultured primary cortical neurons against double-stranded RNA-induced neurotoxicity.
2. Minocycline but not memantine or glycoconjugate protected cultured cells and warrants further investigation.

Introduction

Japanese encephalitis virus (JEV) is an RNA virus spread by infected mosquitoes. Patients may develop symptoms such as fever, chills, tiredness, headache, nausea, vomiting, confusion, and agitation. The disease can lead to serious infection in the brain (encephalitis), and in about 30% of patients severe brain damage ensues. There is no specific treatment for the disease, and the role of medication is to relieve severe symptoms.

Few studies have reported on protection of neurons subsequent to viral infection. We hypothesise that neuroprotective drugs can be used to treat Japanese encephalitis patients and safeguard neurons. We tested some neuroprotective drugs from western and Chinese medicine (minocycline, memantine, and glycoconjugate) for treating Japanese encephalitis. The double-stranded RNA analogue, pIpC, is a commonly used analogue mimicking the consequence of virus infection. Cell cultures of neurons were used to investigate whether these three drugs could attenuate any direct toxic effects of pIpC toward neurons. The underlying mechanisms of the neuroprotective effects were also investigated.

Minocycline is a semi-synthetic tetracycline derivative exhibiting biological effects of neuroprotection in different types of neurological disorders including Parkinson's disease, amyotrophic lateral sclerosis, spinal cord injury, and cerebral ischaemia.[1,2] Such neuroprotective effects are largely attributed to the inhibition of microglia and production of inflammatory factors. Minocycline can even attenuate the excitotoxicity of glutamate in the cerebrospinal fluid from amyotrophic lateral sclerosis patients. The pathology of Japanese encephalitis entails severe cerebral inflammation, which may be minimised by minocycline and so protect neurons.

Memantine is a non-competitive NMDA open channel blocker approved by the US Food and Drug Administration for neuroprotection in Alzheimer's disease.[3] Glutamate is usually released from injured or energy deficient neurons in many neurological disorders. It can further depolarise other healthy neurons and the potassium ions released from such depolarised neurons can enhance cerebral inflammation aggravating neuronal death.[4] Memantine may serve as neuroprotective agent to minimise secondary brain damage exerted by glutamate.

Glycoconjugate is extracted from the anti-ageing Chinese medicine *Lycium barbarum*. It is neuroprotective against the toxicity exerted from β-amyloid protein, a toxin found in the Alzheimer's disease, as well as retinal ganglion cells in an animal model of glaucoma.[5] Its cytoprotective properties may extend to other neurodegenerative diseases and even Japanese encephalitis or its dsRNA-elicited neurotoxicity.

Methods

This study was conducted from 1 June 2006 to 31 May 2008. Protection of

Laboratory of Neurodegenerative Diseases, Department of Anatomy, Research Centre of Heart, Brain, Hormone and Healthy Aging, LKS Faculty of Medicine, The University of Hong Kong
SY Yik, MS Yu, YS Ho, CSW Lai, YT Cheung, KF So, RCC Chang

RFCID project number: 05050032

Principal applicant and corresponding author:
Dr Raymond Chuen-Chung Chang
Department of Anatomy, Faculty of Medicine, The University of Hong Kong, 21 Sassoon Road, Pokfulam, Hong Kong SAR, China
Tel: (852) 2819 9127
Fax: (852) 2817 0857
Email: rcchang@hkucc.hku.hk

neurons from the direct toxic effects of pIpC by the three drugs (minocycline, memantine, and glycoconjugate) was examined, using primary cultures of cortical neurons and human neuroblastoma SH-SY5Y cells. Primary cortical neurons were prepared from embryonic day 17 Sprague-Dawley rats (Laboratory Animal Unit, The University of Hong Kong).[6] In brief, cerebral cortices were mechanically dissociated in phosphate-buffered saline with glucose (18 mM). Cells were seeded onto six-well (0.8×10^6 cells/well) or 12-well plates (1.0×10^5 cells/well) pre-coated with poly-L-lysine (25 µg/mL). The culture medium consisted of Neurobasal Medium supplemented with 2% B-27 supplement, L-glutamine (2 mM), penicillin (50 U/mL), streptomycin (50 µg/mL), and 2-mercaptoethanol. Neurons were maintained at 37ºC in a humidified atmosphere of 5% CO_2 and were cultured for 7 days prior to treatment.

To evaluate whether minocycline exerted neuroprotective effects, neurons were pretreated with different dosages of potential drugs for 1 h prior to exposure of pIpC. Neurons were challenged by 20 µg/mL pIpC with FuGENE 6 reagent. After 48 h, neurons were harvested for assay. General toxicity was determined by measuring lactate dehydrogenase (LDH) activity released into culture medium. Apoptosis was assessed by determining caspase-3 activity. TUNEL and DAPI nuclear staining were used to count the number of apoptotic bodies.

All results obtained were expressed as mean±standard error from at least three independent experiments. Significant difference between groups was determined by one-way ANOVA, followed by Student-Newman-Keuls as a post hoc test.
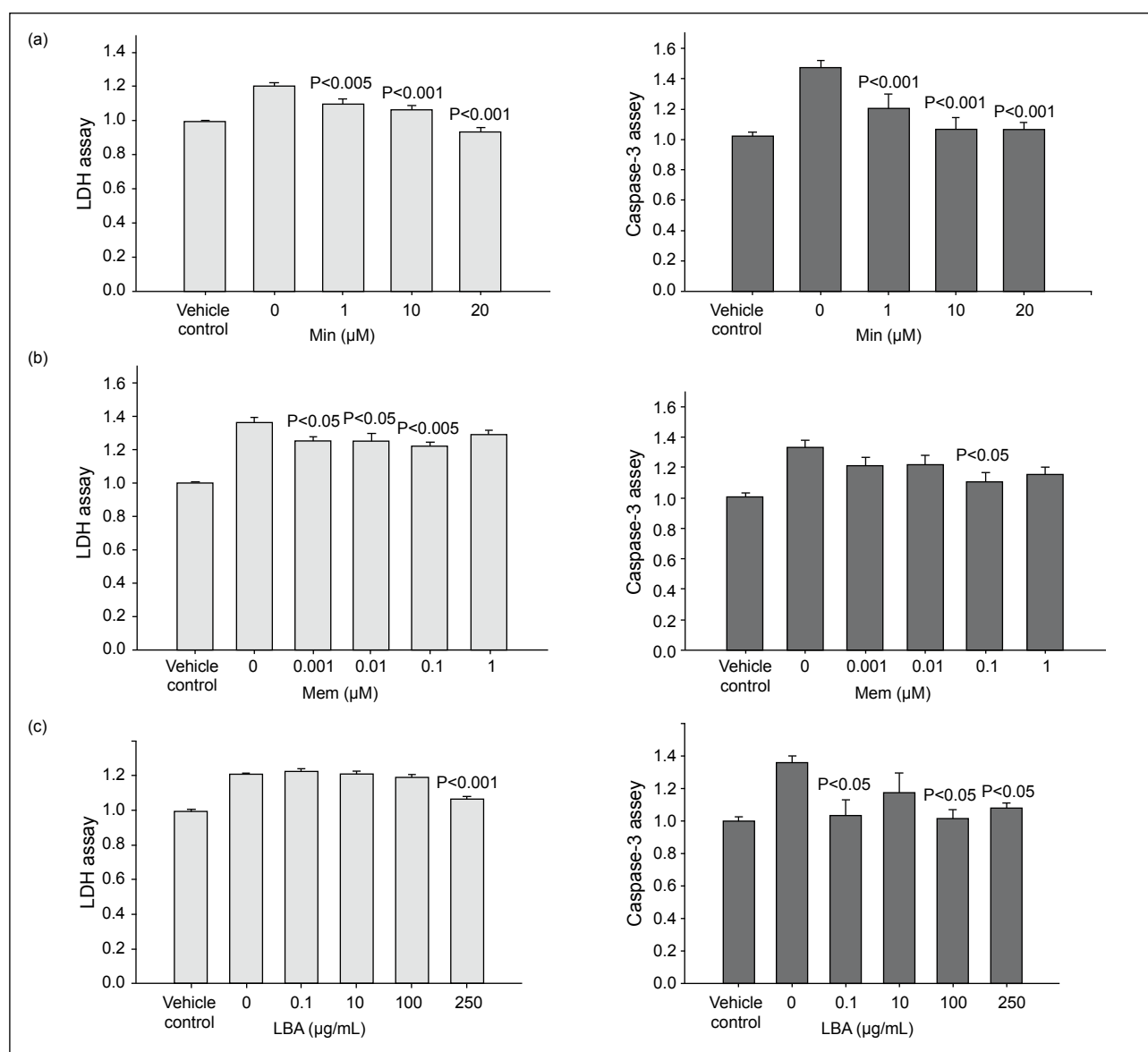
Fig. Effects of minocycline, memantine, and glycoconjugate on pIpC-induced neurotoxicity
Cultured cortical neurons were treated with (a) minocycline, (b) memantine, or (c) glycoconjugate at different dosages 1 h prior to the exposure of 20 µg/mL pIpC. Culture medium was taken for lactate dehydrogenase (LDH) assay and cells were harvested for caspase-3 assay 24 h after treatment

Results and discussion

pIpC exhibits direct neurotoxicity. Increased levels of dsRNA produced from JEV can be toxic to cortical neurons. Dose-dependent and time-dependent experiments were performed using primary cultures of cortical neurons and SH-SY5Y cells as two different models.

Exposure of neurons to 20 μg/mL pIpC resulted in 1.23±0.02-fold increase in the release of LDH when compared to the vehicle control. At higher dosage, the release of LDH decreased to 1.15±0.03-fold. Thus, 20 μg/mL pIpC was chosen for the subsequent experiments. As pIpC could trigger its neurotoxicity via activating caspase-3, a colorimetric caspase-3-like activity assay was carried out for different dosages of pIpC. Exposure of neurons to 20 μg/mL pIpC significantly increased the activity of caspase-3 to 1.33±0.06-fold.

Apart from biochemical assays, neurites were damaged by pIpC, as shown by their morphology. Under a phase contrast microscope, the cell bodies of cultured neurons in the control group appeared round and dark with a network of process. After exposure to pIpC, cultured neurons were damaged and showed fragmented neurites.

Exposure of neurons to 20 μg/mL pIpC for 48 h resulted in 1.2±0.03-fold increase in the release of LDH when compared to the vehicle control. There was a slight decrease of LDH release at 72 h. The colorimetric caspase-3-like activity assay was also carried out after different durations of exposure to pIpC. Exposure of neurons to 20 μg/mL pIpC for 48 h significantly increased the activity of caspase-3 to 1.43±0.03-fold. Similar to the results of the LDH release assay, caspase-3-like activity decreased at 72 h. As the maximum increase of LDH release and caspase-3 was at 48 h, this duration was chosen for the subsequent experiments.

Exposure of human dopaminergic SH-SY5Y cell neurons to 20 μg/mL pIpC resulted in 1.50±0.09-fold increase of LDH release when compared to that of the vehicle control. Exposure of neurons to 20 μg/mL pIpC significantly increased the activity of caspase-3 to 1.29±0.03-fold. These results provided further proof of the toxicity of pIpC, using SH-SY5Y cells as second cell culture model.

pIpC induced neuronal apoptosis can be confirmed by recognised methods. Treatment with pIpC for 48 h increased the number of apoptotic bodies (typical nuclear condensation and fragmentation) as indicated by the increased number of TUNEL-positive neurons. TUNEL assay relied on the detection of fragmented DNA strands. In control cultures treated with vehicle, only few TUNEL-positive cells were observed.

Minocycline exhibited the best neuroprotective effect on neurons based on the LDH assay; 10 or 20 μM exerted similar neuroprotection on caspase-3 activity (Fig a). We could not further increase the concentrations of minocycline as this would exceed the normal dosage for treatment and exert side-effect in patients. Memantine significantly reduced the toxicity of pIpC (both LDH release and caspase-3 activity), but its neuroprotective effect was marginal. In contrast to memantine, minocycline elicited significant neuroprotective effects on cortical neurons against direct pIpC toxicity (Fig b). Glycoconjugates from *L barbarum* elicited cytoprotective effects; *L barbarum* attenuated caspase-3 activity triggered by pIpC (Fig c). Nonetheless, only the highest dosage of *L barbarum* could inhibit LDH release triggered by pIpC.

Of the three different compounds, minocycline exhibited significant neuroprotective effects against direct pIpC neurotoxicity and warrants further investigation.

References

1. Tikka TM, Koistinaho JE. Minocycline provides neuroprotection against N-methyl-D-aspartate neurotoxicity by inhibiting microglia. J Immunol 2001;166:7527-33.
2. Tikka TM, Vartiainen NE, Goldsteins G, et al. Minocycline prevents neurotoxicity induced by cerebrospinal fluid from patients with motor neurone disease. Brain 2002;125:722-31.
3. Miguel-Hidalgo JJ, Alvarez XA, Cacabelos R, Quack G. Neuroprotection by memantine against neurodegeneration induced by beta-amyloid (1-40) Brain Res 2002;958:210-21.
4. Chang RC, Hudson PM, Wilson BC, Liu B, Abel H, Hong JS. High concentrations of extracellular potassium enhance bacterial endotoxin lipopolysaccharide-induced neurotoxicity in glia-neuron mixed cultures. Neuroscience 2000;97:757-64.
5. Chang RC, So KF. Use of anti-aging herbal medicine, Lycium barbarum, against aging-associated diseases. What do we know so far? Cell Mol Neurobiol 2008;28:643-52.
6. Lai CS, Yu MS, Yuen WH, So KF, Zee SY, Chang RC. Antagonizing beta-amyloid peptide neurotoxicity of the anti-aging fungus Ganoderma lucidum. Brain Res 2008;1190:215-24.

S Riley
GM Leung 梁卓偉
LM Ho 何禮明
BJ Cowling 高本恩

Transmission of Japanese encephalitis virus in Hong Kong

. . . .

Key Messages

1. Pigs are likely to be the main amplifying host for Japanese encephalitis virus.
2. The success of a swine vaccination programme depends on the timing of the loss of maternal antibody protection and seasonal dynamics of the vector population.
3. Vaccination may be ineffective in the face of strong natural infection because of the variability in timing of the loss of maternal antibody protection.
4. Evidence in support of swine vaccination as a human health intervention was not found.

Background

Local acquisition of Japanese encephalitis virus (JEV) was a regular, if not widespread, occurrence in Hong Kong prior to 1991. Although there have been only seven such cases since then, six of them occurred in 2003/4. The JEV is an indirectly transmitted zoonotic virus. In Hong Kong, the vector is likely to be *Culex tritaeniorhynchus* and the vertebrate amplifying hosts are pigs and wild wetland birds (egrets and herons). Humans are non-amplifying hosts for JEV; they are not able to infect susceptible mosquitoes. Transmission between these species is the main concern for an effective JEV control policy.

Based on a mathematical model, the role of transmission involving the vector and amplifying hosts was assessed.[1] Pigs are the principal source of JEV infection in mosquitoes. This suggests swine vaccination may be a strategy for preventing human infection. However, the seasonal variation in mosquito population drives most of the dynamics of JEV transmission. The lack of vector data precludes prediction of the impact of any vaccination programme.

We aimed to describe quantitatively the role of mosquitoes, pigs, and wild birds in the transmission of JEV in Hong Kong, and assess more accurately the likely impact of swine vaccination.

Methods

This study was conducted from 1 September 2006 to 17 August 2007. Four distinct deterministic compartmental models were used, one each for mosquitoes, pigs, wild birds, and humans with various transmission processes: susceptible, exposed, infectious, and recovered. Transmissions were linked by the mosquito-biting event.

Seasonal variation in the mosquito population was assumed to have exponential growth and decay in spring and fall, respectively. Decrease in maternal antibody protection in pigs and their age structure were modelled to allow realistic assessment of swine vaccination. Transmission under two scenarios (different duration of summer peak vector season) was simulated, consistent with mosquito data.

Relevant estimates from the literature were used for parameters such as lifespan of JEV vectors, their expected number of blood meals, and duration of infectiousness in pigs. Local ovitrap data for the species *Aedes albopictus* were used as a proxy for the seasonal variation in JEV vector population.

Data for JEV seroprevalence in pigs were collected, which showed marked seasonal trends over years. These were used to calibrate the transmission model after which the impact of a swine vaccination programme was assessed.

Results

An optimised two-dose swine vaccination strategy is likely to be effective if the peak summer period is very short and the winter vector population is large. However, swine vaccination is likely to have little effect if the summer season is much longer and the winter vector population is smaller. In both scenarios,

Department of Community Medicine and School of Public Health, The University of Hong Kong
S Riley, GM Leung, LM Ho, BJ Cowling

RFCID project number: 05050132

Principal applicant and corresponding author:
Dr Steven Riley
School of Public Health, The University of Hong Kong, LKS Faculty of Medicine Building, 21 Sassoon Road, Pokfulam, Hong Kong SAR, China
Tel: (852) 2819 9280
Fax: (852) 2855 9528
Email: s.riley@imperial.ac.uk

excess human JEV infection attributed to transmission by wild birds is <20%.

Conclusions

Interaction of a maternal antibody protection in a non-seasonal pig population and a highly seasonal vector population makes the likely success or failure of swine vaccination difficult to predict. Nonetheless, an optimised two-dose vaccination for pigs would have a dramatic decrease on the number of human infection caused by pigs if the peak vector season is short. Further field studies should systematically quantify the abundance of potential vectors, their rates of viral carriage, and identification of the mosquito blood meals. This would enable a direct estimate of the relative biting probabilities in the model. Moreover, the contribution of wild bird in human JEV infection is minor.

Reference

1. S Riley. A comprehensive risk assessment of Japanese encephalitis in Hong Kong using mathematical modeling. Dissemination report No. HKU-AA-009. Food and Health Bureau. 2004. Available from http://fhbgrants.netsoft.net/report/HKU-AA-009.pdf. Accessed 1 November 2011.

AUTHOR INDEX